UNITED NATIONS UNIVERSITY
GEOTHERMAL TRAINING PROGRAMME
Orkustofnun, Grensasvegur 9,
IS-108 Reykjavik, Iceland

Reports 2012
Number 32

JOINT 1D INVERSION OF MT AND TEM RESISTIVITY DATA FROM THE THEISTAREYKIR HIGH-TEMPERATURE GEOTHERMAL AREA, NE-ICELAND AND COMPARISON WITH ALTERATION AND TEMPERATURE LOGS FROM BOREHOLES

Nuwan Buddika Suriyaarachchi
Institute of Fundamental Studies
Hanthana Road
Kandy
SRI LANKA
nuwan@ifs.ac.lk, nuwan1985@gmail.com

ABSTRACT

Due to future demands for energy, it is essential to identify and develop new geothermal fields. As a result of this situation, many exploration projects have been carried out. Magnetotelluric (MT) and Transient electromagnetic (TEM) soundings in Theistareykir area were carried out by Iceland Geo-Survey (ISOR). In this study 15 MT and 15 TEM soundings from Theistareykir were used to study the resistivity subsurface structure. Both 1D TEM inversion and MT-TEM joint 1D inversion were performed for each and every sounding site. Two resistivity profiles and a number of iso-resistivity maps were compiled. With the aid of Z-strike, T-strike analysis and alteration mineralogical data from neighbouring boreholes, the resistivity structure and possible heat sources were interpreted.

1. INTRODUCTION

1.1 Geophysical measurements of geothermal areas

Geophysical surveys measure variations of physical phenomena such as electric fields, magnetic fields and gravity, etc. These surveys can be considered a key to unlocking the secrets of the earth without major excavation. Most of geophysical exploration methods specialize in particular properties. But each method contributes considerably in geothermal energy exploration.

Geophysical exploration is a major phase in geothermal resource exploration. Electromagnetic (EM) methods play a big role in modern exploration. Transient Electromagnetic method (TEM) and magnetotellurics (MT) play a big role in geothermal exploration and monitoring. Electromagnetic methods measure subsurface resistivity. According to a resistivity profile, a basic conceptual model is defined and a final model is obtained as a result of complex processing and calculations. These resistivity models can be used to find subsurface structures and related properties such as salinity, porosity, alteration, temperature, etc.

The combined use of TEM and MT has been found to be a very good tool for exploring geothermal resources. The MT method has been used for over 7 decades with growing accuracy. In this modern

age, it has achieved vast advancements with the aid of powerful computing facilities. Modelling and interpretation have become more elaborate and easier with powerful computers and now 3D interpretation methods are starting to play a big role.

1.2 General description of Theistareykir area

The Theistareykir geothermal field is located in NE-Iceland (Figure 1). It has been a well-known geothermal area for a long time. For centuries sulphur was mined and processed there. It delivered a promising income to the Danish king, providing good raw material for gun powder. According to legend, 12 polar bears came to the Theistareykir area and plagued the farmers living around there. One of the farmer's sons chased them and killed them all. There is also a story about a ghost which haunted the farm there. The farm was abandoned in the early 1870s, and it is now a shelter for sheep farmers during the round-ups. Former farm land is located adjacent to some of the surface manifestations, such as boiling mud ponds; these manifestations prove that there is an underlying high-temperature system.

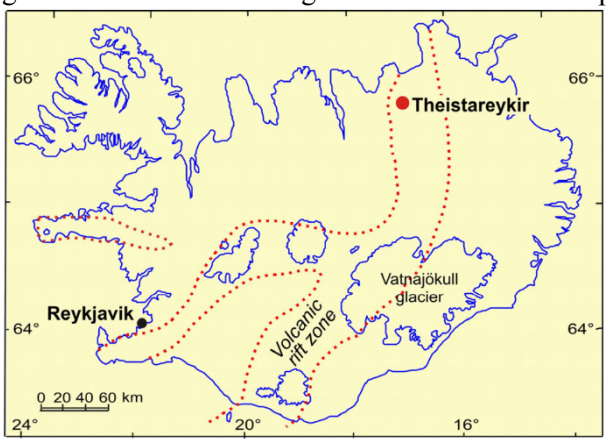

FIGURE 1: Location of the Theistareykir area

Iceland is widely accepted to be underlain by the plume of an upwelling hot mantle (Morgan, 1971; Schilling et al., 1982). The high-temperature geothermal area of Theistareykir lies on the northern side of its proposed location. The Theistareykir fissure swarm forms the northernmost segment of the Northern rift zone, a mature rift undergoing active spreading. In this northern region of the active rift zone, the tectonic regime is relatively simple, with rifts running north-south, orthogonal to the spreading direction (Slater et al., 2001).

Theistareykir is one of the high-temperature geothermal areas feasible for future exploitation. During the summer of 2002, a few experimental boreholes were drilled in the area to test the capacity of the high-temperature area for future exploitation. Researchers suggested that it was realistic that a 150 MWe electrical power plant could be built in the area. Thorough explorations were conducted in the Theistareykir area during 1972-1974 and 1981-1983, and 7 deep boreholes have been drilled there since 2002. Vast amounts of data were collected through continuous well testing, on the pressure and temperature conditions in the geothermal system, as well as pressure transient data, which can be used to estimate permeability.

2. SOME FUNDAMENTALS

The chapter briefly describes fundamentals such as wave theory which is the basis for electromagnetic methods and resistivity measurements. Also, variations in resistivity, based on rock properties, are briefly discussed. Furthermore, understanding resistivity data and temperature correlations is addressed.

2.1 Resistivity of rocks

Resistivity measurements can be used to create a good picture of underlying structures. Most pressure and temperature dependent chemical reactions contribute to variations in electrical resistivity. Mineral alteration, secondary mineralization, porosity changes, and pore fluid compositional changes accommodate widely ranged resistivity values even in the same rock formation. Also some physical reactions such as tectonic activities, pressure changes and temperature changes play their own roles to

change electrical resistivity, even in the same chemical composition. In other words, both chemical and physical variations directly affect the electrical resistivity of rocks.

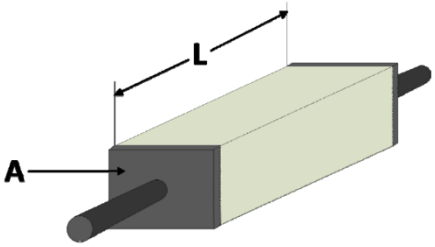

FIGURE 2: Resistivity and parameters (see Equation 1)

Electrical resistivity of a material can be defined by its physical parameters. In reality, resistivity of water bearing rock formations behaves in a slightly different way, depending on both the matrix and fluid resistivity. If current is transmitted through an elongated rectangle and then the potential measured across it (Figure 2), the following equation describes resistivity (Ωm):

$$\rho = \frac{\Delta V}{I}\frac{A}{L} = R\frac{A}{L} \tag{1}$$

where ρ = Specific resistivity of the material (Ωm);
R = Electrical resistance of the material (Ω);
ΔV = Potential difference (V);
I = Electrical current (A);
L = Length (m);
A = Cross-section area of conducting (m^2)

Rearranging the above equation, we can derive the relationship between the electric field's strength and the current density as follows:

$$\frac{\Delta V}{L} = \rho\,\frac{I}{A} \quad or \quad E = \rho j \tag{2}$$

where E = Electric field strength (V/m)
j = Current density (A/m^2)

2.2 Electrical resistivity versus temperature and alteration

Fluid presence in a rock matrix often causes drastic changes in electrical resistivity. For moderate temperatures, 0-200°C, the resistivity of aqueous solutions was estimated by Dakhnov (1962) as follows:

$$\rho_w = \frac{\rho_{w_0}}{1 + \alpha(T - T_0)} \tag{3}$$

where ρ_w = Resistivity of fluid at temperature T (Ωm);
ρ_{w_0} = Resistivity of fluid at temperature T_0 (Ωm);
α = Temperature coefficient of resistivity ($°C^{-1}$),
$\alpha \approx 0.023\ °C^{-1}$ for T_0 = 23°C and $0.025°C^{-1}$ for T_0 = 0°C;
T_0 = Reference temperature (°C).

Increasing mobility of dissolved ions contributes to reducing resistivity with increasing temperature (Figure 3). But above 300°C, electrolyte resistivity starts to increase with temperature, because a decrease of the dielectric permittivity of water results in a decrease in the number of dissociated ions in the water (see Figure 3).

A rock matrix accommodates pore fluids in three ways, namely: intergranular (pores between the grains), joints-fissures (net of fine fractures), and vugular (irregular pores formed by gas or dissolved minerals). Discontinued fractures and pores do not contribute to electrical conduction. Fractional porosity is defined as follows:

$$\phi_t = \frac{V_\varphi}{V} \tag{4}$$

where ϕ_t = Fractional porosity;
V_φ = Volume of voids (m^3)
V = Total volume of material (m^3)

Permeability is the measure of fluid circulation inside solid rock. Though rock is highly porous, most of the porous rock may not facilitate fluid flow. Therefore, the concept of effective porosity becomes very significant. The effective porosity represents the interconnected network of pores and fractures. Sometimes, fractures are major components for effective porosity. In addition, the host material characteristics, fluid viscosity and fluid pressure, can also affect pore-fluid flow.

If fluid conduction dominates Equation 5, also known as Archie's empirical law, can be used to describe bulk resistivity:

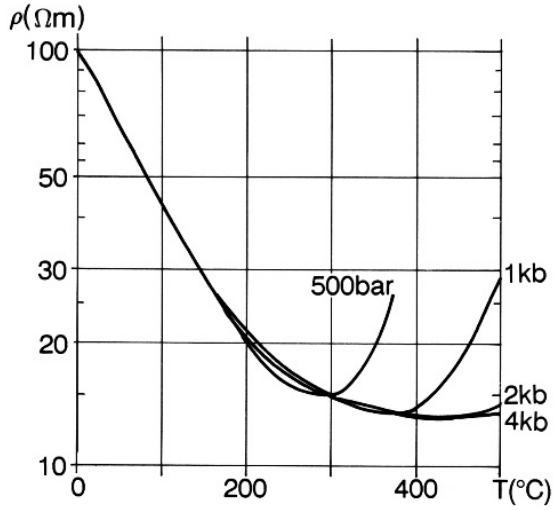

FIGURE 3: Electrical resistivity of NaCl solutions as a function of temperature at different pressures (Hersir and Björnsson, 1991, modif. from Quist and Marshall, 1968)

$$\rho = \rho_w \, a \, \phi_t^{-m} \tag{5}$$

where ρ = Bulk resistivity (Ωm);
ρ_w = Resistivity of pore fluid (Ωm);
ϕ_t = Fractional porosity;
a = Empirical parameter, usually around 1;
m = Cementing factor, an empirical parameter which varies from 1.2 for unconsolidated sediments to 3.5 for crystalline rocks, usually around 2.

Equation 5 can also be expressed as:

$$\rho = \rho_w F \tag{6}$$

where F is known as the formation factor: $F = a \, \phi_t^{-m}$

Rocks do not allow us to use simple formulas to describe their chemical properties. Wide variations of metals, oxides, sulphides, sulphates, silicates, aluminates, phosphates and other minerals create endless chemical variety for rocks. Also, these minerals change their chemical composition and form new materials, called alteration minerals. Alteration minerals are key products for determining temperature. The intensity of the alteration depends on temperature, time and host rock texture. Well known resistivity structures for high-temperature fields in Iceland are shown in Figure 4. Alteration intensity is very low for temperatures below 50-100°C. And at the same time, resistivity is fairly high. The alteration mineral formation increases with increasing temperature, causing decreasing resistivity. Smectites-zeolites are dominant up to 200°C (Pytte and Reynolds, 1989; Tucker, 1991). The zeolites are silicates consisting of interlocking tetrahedrons of SiO_4 and AlO_4. The alumino-silicate structure is negatively charged and attracts positive cations that reside within it. Unlike most other tecto-silicates, zeolites have large vacant spaces or cages in their structures which have space for large cations such as sodium, potassium, barium and calcium and even relatively large molecules and cation groups such as water, ammonia, carbonate ions and nitrate ions.

The clay mineral smectite is a sheet silicate with inter-layered cations which are mostly exchangeable. The principal reason for cation exchange is the imbalance of charge in the fundamental layers, but some

additional exchange could take place through deficient valences. Due to the high inter-layer distance of water, most of the ions and even organic cations can pass through. Upon heating, the inter-layered water of smectite is lost, mostly between 100 and 250°C, but some remains to about 300°C (Deer et al., 1962).

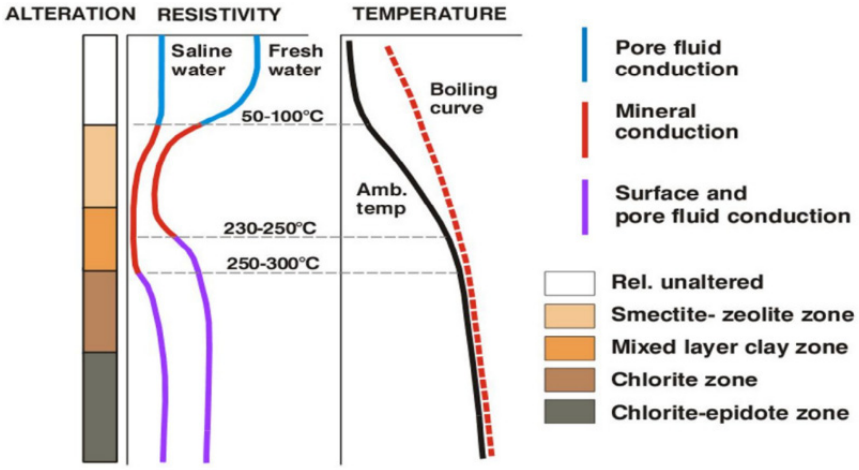

FIGURE 4: General resistivity of high-temperature fields in Iceland (Flóvenz et al., 2012)

Figure 5 shows the mineral alteration zones vs. temperature. In the smectite-zeolite alteration zone, mineral conduction becomes the dominant conduction mechanism. Below the smectite zone, resistivity increases due to the strongly reduced cation exchange ability in clay layers. Mixed-layer clay and chlorite become dominant in this zone. In this zone, surface and pore fluid conduction probably dominates as the mineral conduction is weakened. The transition from smectite to mixed-layer clay happens at a temperature of around 230-250°C, and there we have the high-resistivity core with temperatures higher than 250°C where alteration minerals like chloride and epidote are present.

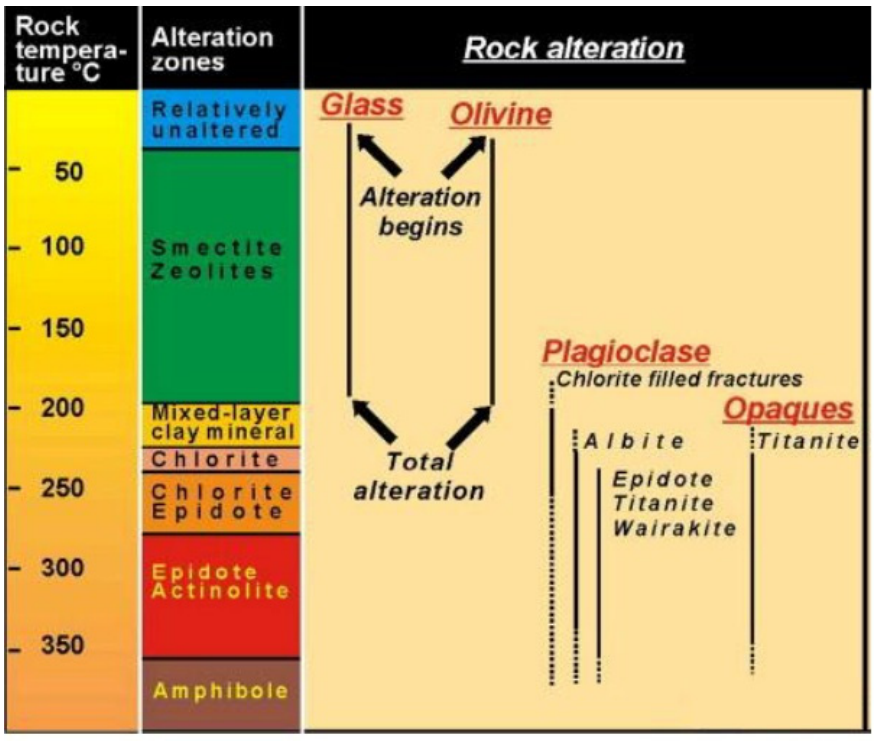

FIGURE 5: Mineral alteration – temperature diagram (modified from Franzson, 2008)

In some cases the alteration temperature can differ from the formation temperature. That difference can express the dynamic state of the geothermal system, such as cooling. If the alteration and temperature are in equilibrium, the resistivity structure reflects not only the alteration but also the temperature, but it can be considered a maximum thermometer.

2.3 Electromagnetic wave propagation

Easy to use and with enhanced resolution, electromagnetic methods are finding increasing usage in many exploration applications, such as environmental, engineering and archaeological exploration. These

methods are based on: Ampère's law, Gauss's law and Faraday's law. With modern technology, these methods became more common and began to be used for day to day human needs.

Electromagnetic waves and geophysical exploration methods combined since the 1950s. Cagniard (1953) and Tikhonov (1950) developed the first electromagnetic method, the natural source MT, with the aid of Maxwell's equations which derived from Ampère's, Gauss's and Faraday's laws. As we know, all electromagnetic waves have both electric and magnetic properties; Maxwell's equation describes the relationship between electric and magnetic components.

Electromagnetic (EM) waves, in vacuum, move at the speed of light. The velocities of EM waves in the ground are less than the speed of light, but are still very fast. For typical EM measurements at a frequency of 10 kHz, and using the speed of light of 3×10^8 ms^{-1}, the wavelength can be calculated to be of on the order of 30 km. In general, geophysical instruments use very long wave lengths. Therefore, EM surveying wave lengths are so much longer than the survey area that the field is effectively the same over the entire area, and only the time varying properties of the field need to be considered. EM wave propagation is influenced by the electrical properties of the material through which it propagates. The material's properties directly affect to efficiency of the propagation, the loss of energy within the medium, and the speed of propagation.

1. *Faraday's law* states that an electric field is produced by a time varying magnetic field:

$$\nabla \times \boldsymbol{E} = -\mu \frac{\partial \boldsymbol{H}}{\partial t} \tag{7}$$

2. *Ampère's law* states that a magnetic field is produced by an electric current or by a time varying electric field:

$$\nabla \times \boldsymbol{H} = \boldsymbol{j_c} + \frac{\partial \boldsymbol{D}}{\partial t} \tag{8}$$

3. Gauss's law relates an electric field to its source charges:

$$\nabla \cdot \boldsymbol{D} = Q \tag{9}$$

where $\boldsymbol{D}$ is the electric field displacement and Q is the electric charge density.

Similarly, for the magnetic field:

$$\nabla \cdot \boldsymbol{B} = 0 \tag{10}$$

Other relationships are:

$$\boldsymbol{J} = \sigma \boldsymbol{E} \tag{11}$$

$$\boldsymbol{B} = \mu \boldsymbol{H} \tag{12}$$

$$\boldsymbol{D} = \varepsilon E \tag{13}$$

where ε, μ, and σ are dielectric permittivity, magnetic permeability and electric conductivity, respectively.

3. TRANSIENT ELECTROMAGNETIC AND MAGNETOTELLURIC METHODS

When dealing with EM waves, as a means for exploration, there are two options, i.e. use of man-made sources or natural sources. Transient electromagnetic methods or time domain electromagnetic (TEM) methods are active methods with a man-made source, ideal for most shallow exploration activities; the magnetotelluric method, a passive (natural source) method, is ideal for much greater depths.

3.1 The transient electromagnetic methods (TEM)

Transient electromagnetic method (TEM) is a very popular method among geophysicists due to its very good imaging properties. It is extensively used not only in geothermal exploration, but also groundwater, mineral and archaeological exploration and for many other purposes. The TEM method has gained popularity since the 1980s. This method is easy to use even where the use of the Schlumberger method is limited.

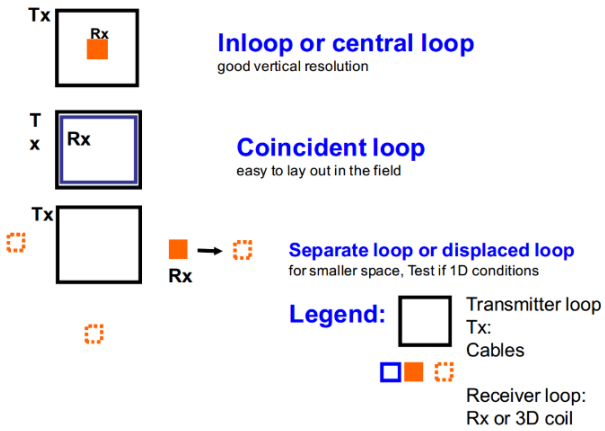

FIGURE 6: Different layouts of transmitter and receiver loops for TEM measurements

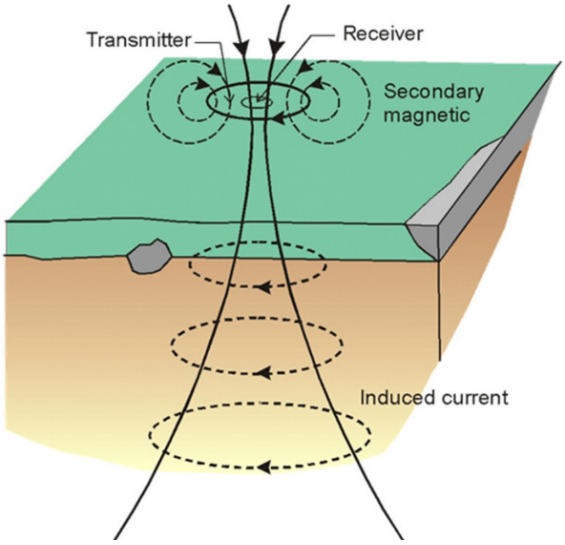

FIGURE 7: The central loop TEM electric-magnetic field generation

The TEM method uses a controlled source transmitter and a receiver. With regard to receiver loop positioning, there are three main configurations (Figure 6), namely central loop layout, a coincident loop and a displaced loop. The TEM method uses induced currents in the ground, caused by primary electromagnetic waves from a transmitter loop. The central loop layout is effective in measuring the vertical component of the induced magnetic field. Due to its simple layout of receiving and transmitting loops, a relatively small work force is needed and good readings can be obtained effectively and repeatedly without changing the field layout. TEM responses are more downward focussed. The TEM method does not need any current to be injected into the earth; therefore, the method can be used in all accessible terrains, regardless of surface conditions, such as on snowy, rugged mountains or dry sand surfaces, without affecting the electromagnetic signatures. The combination of several soundings along a profile may give 2D variations of the subsurface.

In the central loop method, a transmitting loop is placed on the ground and a constant magnetic field with known strength is built up by transmitting a constant current into the transmitting loop (Figure 7). First, a constant DC current is transmitted into the transmitting loop to generate a constant magnetic field of known strength around the loop. The current is then abruptly turned off. Once the current is switched off, the decaying magnetic field induces electrical currents into the ground to compensate for the effects. The induced electric field, on the other hand, produces a secondary magnetic field decaying with time. The production of secondary electromagnetic fields in the absence of primary sources is called a transient electromagnetic wave (TEM-wave). The decay rate of the secondary magnetic field is monitored by measuring the voltage induced in the receiver coil. For repeated measurements, the transmitter has to be switched off and on at a set interval or in predetermined frequencies (Figure 8).

The transmission of a TEM signal can be looked at as a signal spike train with a particular frequency. Signals sent in both + and – directions to avoid polarization of the conducting bodies. The response of the ground is detected at predefined time gates during current-off time. The strength of the magnetic force injected into the earth depends upon the transmitted current and the number of turns; this is also called the effective area:

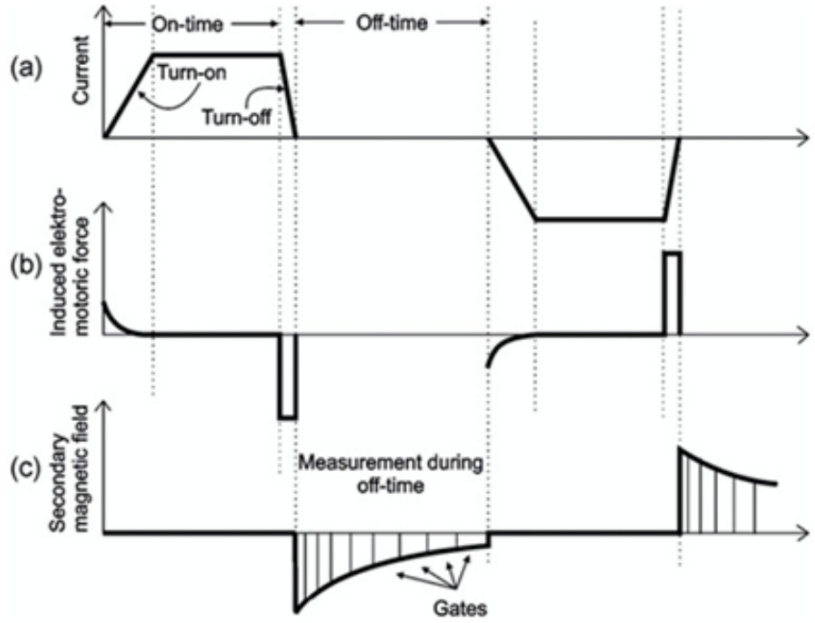

FIGURE 8: TEM measurements, (a) Current flow in the transmitter loop; (b) Induced electromagnetic force in the ground; c) The secondary magnetic field measured at time gates (Christensen et al., 2006)

$$\text{Effective area} = \text{area surrounded by loop} \times \text{number of windings}$$

A detailed mathematical description of the central-loop TEM method is somewhat complicated. The following equations were developed by Árnason (1989). The problem is solved using reciprocity and considering a vertical magnetic dipole source of magnetic moment (***M***) at point x:

$$\boldsymbol{M} = \boldsymbol{M}_0\, e^{i\omega t}\boldsymbol{z}\delta(\boldsymbol{x}-\boldsymbol{x_0}) \tag{10}$$

where $\boldsymbol{M}_0$ = Initial magnetic dipole moment;
z = Unit vector;
δ = Dirac´s delta function.

Voltage response induced in a circular receiver loop of radius r_c around the dipole is:

$$V_c = 2\pi n_r r_c E(r_c) = A_r n_r \frac{2E\,(r_c)}{r_c} \tag{15}$$

The mutual coupling of the voltage in the receiver and the transmitter defines the mutual impedance of the subsurface as expressed in Equation 16:

$$Z_c\,(r,\omega) = \frac{V_c}{I_0 e^{\,i\omega t}} = A_r n_r A_s n_s \frac{-i\omega\mu_0}{\pi r}\int_0^\infty \frac{\lambda^2}{m_0}\frac{S_0}{S_0 - T_0}J_1(\lambda r)d\lambda \tag{16}$$

where S_0 and T_0 contain the parameters of the layered earth, and are determined by the recurrent relationship:

$$S_{i-1} = S_i\, cosh(m_i d_i) - T_i \sinh(m_i d_i) \tag{17}$$

$$T_{i-1} = -\frac{m_i}{m_{i-1}}[S_i \sinh(m_i d_i) - T_i cosh(m_i d_i)] \tag{18}$$

$$S_{N-1} = 1 \tag{19}$$

$$T_{N-1} = -\frac{m_N}{m_{N-1}} \tag{20}$$

$$m_i = \sqrt{\lambda^2 - k_i^2} \tag{21}$$

$$k_i^2 = \omega^2 \mu\varepsilon - i\omega\mu\sigma_i \tag{22}$$

where d_i = Thickness of the i^{th} layer (m);
m_i = Impedance of the i^{th} layer;
σ_i = Conductivity of the i^{th} layer (S/m).

The Fourier expansion of the transmitted current function *I(t)* is:

$$I(t) = \frac{1}{(2\pi)^{1/2}} \int_{-\infty}^{\infty} \bar{\mathrm{I}}(\omega) e^{i\omega t}\, d\omega \tag{23}$$

where, I(ω):

$$\bar{\mathrm{I}}(\omega) = \frac{1}{(2\pi)^{1/2}} \int_{-\infty}^{\infty} I(t)\, e^{-i\omega t} dt \tag{24}$$

The response of the measured voltage in terms of the mutual impedance as a function of time for a homogeneous earth is:

$$V_c(t,r) = \frac{1}{(2\pi)^{1/2}} \int_{-\infty}^{\infty} Z_c\,(\omega, r)\bar{\mathrm{I}}(\omega) e^{i\omega t}\, d\omega \tag{25}$$

$$V_{(t,r)} \approx I_0 \frac{C\ (\mu_0\, \sigma\, r^2)^{3/2}}{10\ \pi^{1/2} t^{5/2}} \tag{26}$$

where

$$C = A_r n_r A_s n_s \frac{\mu_0}{2\pi r^3}$$

Apparent resistivity, ρ_a, in terms of induced voltage at late times after the source current is turned off is defined by (Árnason, 1989):

$$\rho_{a=} = \frac{\mu_0}{4\pi}\left[\frac{2\ \mu_0 A_r n_r A_s n_s I_0}{5\ t^{5/2} V_c(r,t)}\right]^{2/3} \tag{27}$$

where t = Elapsed time after the transmitter current is turned off (s);
A_r = Cross-sectional area of the receiver coil (m^2);
n_r = Number of windings in the receiver coil;
μ_0 = Magnetic permeability in vacuum (H/m);
A_s = Cross-sectional area of the transmitter loop (m^2);
n_s = Number of windings in the transmitter loop;
I_0 = Transmitter current (A);
V(r,t) = Measured voltage (V);

The time behaviour of the voltage response for different resistivity has the same character and can be divided into three phases: early times, intermediate times and late times. The induced voltage is constant at the early stage and starts to decrease with time in the intermediate stage. At late times, the measured voltage *V(t)* decays over time in such a way that the logarithm of the induced voltage decreases linearly as a function of the logarithm of time, and in this last stage the slope of the curve is – (5/2), showing that the voltage is proportional to $t^{-5/2}$ and varies as $\sigma^{3/2}$ (Equation 26) (Figure 9). Also, the early time response depends on resistivity, because it increases as resistivity increases. There is a variation (stages are shifted) in the transition from early time to intermediate and from intermediate to late time, depending on the resistivity.

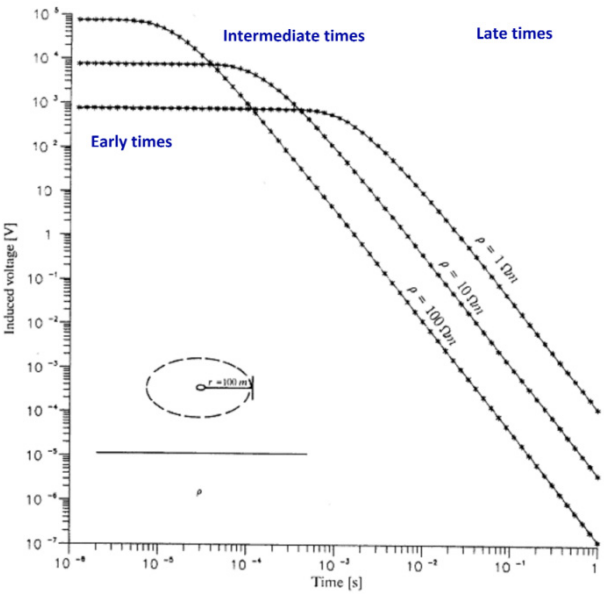

FIGURE 9: Voltage response for a homogeneous half-space (modified from Árnason, 1989)

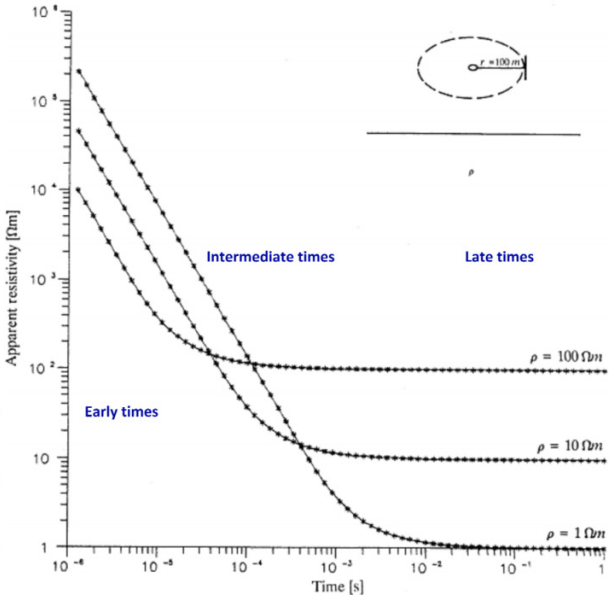

FIGURE 10: Late time apparent resistivity for a homogeneous half-space (modified from Árnason, 1989)

Apparent resistivity, ρ_a, of a homogeneous half-space, in terms of induced voltage at late times after the source current is turned off, is given by Árnason (1989), shown in Figure 10.

3.2 The magnetotelluric (MT) method

The magnetotelluric (MT) method is a passive method. It uses naturally occurring electromagnetic waves and measures both the electric (**E**) and magnetic (**B**) field in orthogonal directions (Figure 11). This method is a convenient means for determining the conductivity structures at depths ranging from a few tens of metres to hundreds of kilometres.

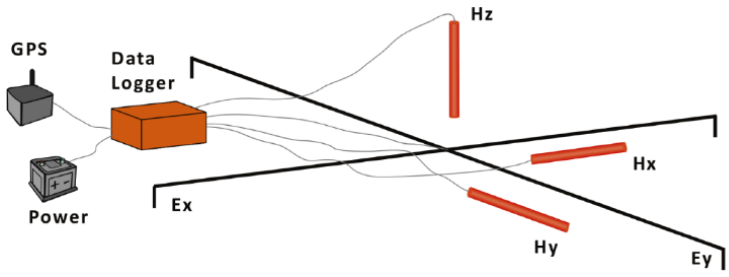

FIGURE 11: Basic configuration for MT sounding

In the 1950s, the most fundamental theory of exploration MT was propounded by Tikhonov (1950), but later it was given in more detail by Cagniard (1953). For a homogeneous earth, can be determined by the ratio of the orthogonal electric, ***E***, and magnetic, ***B***, fields:

$$\rho = \frac{1}{\omega\mu}\left|\frac{\boldsymbol{E}}{\boldsymbol{H}}\right|^2 = 0.2\left|\frac{\boldsymbol{E}'}{\boldsymbol{B}''}\right|^2 \qquad (28)$$

where ω = Angular frequency ($2\pi f$);
μ = Magnetic permeability (H/m);
$\boldsymbol{E}$ = Electric field (V/m);
$\boldsymbol{H}$ = Magnetic intensity (A/m);
$\boldsymbol{E}'$ = Electrical field (mV/km);
$\boldsymbol{B}'$ = Magnetic induction (nT), $\boldsymbol{B}' = \mu\,\boldsymbol{H} \times 10^{-9}$.

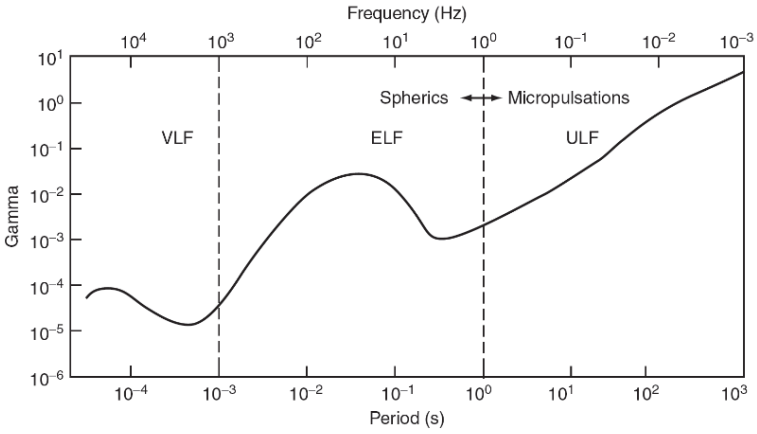

FIGURE 12: The natural magnetic field spectrum

The high frequencies give information about the resistivity at shallow depths while the low frequencies provide information about the deeper lying structures. The small-amplitude geomagnetic time variations of Earth's electromagnetic (EM) field contain a wide spectrum generated by two different sources. The low frequencies are produced by ionospheric and magnetospheric currents caused by the solar wind emitted from the sun interfering with the Earth's magnetic field; these are known as micro-pulsations. Higher frequencies, > 1 Hz, are produced by thunderstorm activity near the equator and are distributed as guided waves, known as sferics, between the ionosphere and Earth, to higher latitudes. The natural EM fluctuations of interest here have two relatively low-intensity ranges, the so-called dead-band. The MT 'dead-band' is at approximately 0.5–5 Hz (2–0.2 s) and the audio magnetotelluric (AMT) 'dead-band' is at approximately 1–5 kHz. MT and AMT measurements in these frequency ranges usually suffer from poor data quality, resulting in high uncertainties for data for a certain depth interval (Figure 12).

Penetration depth or the electromagnetic skin depth, δ, is a key concept for describing the relationship between conductivity and depth of exploration. The electromagnetic field has attenuated to e^{-1} of the amplitudes at the surface of the earth at δ depth. The skin depth for a homogeneous earth is as follows:

$$\delta = 500\sqrt{T\rho} \tag{29}$$

where δ = Skin depth (m);
ρ = Resistivity, or the average resistivity of an equivalent uniform half-space (Ωm)
T = Period (s).

A number of assumptions have to be made to simplify the behaviour of electromagnetic induction in the earth:

- All source fields, generated far from the earth's surface, may be treated as uniform, and all plane polarized electromagnetic waves impinging on the earth have near vertical incidence.
- No accumulation of free charges is expected to be sustained within a layered earth. In a multidimensional earth, charges can accumulate along discontinuities. This generates a non-inductive phenomenon known as static shift.
- The earth behaves as an ohmic conductor, obeying:

$$j = \sigma E \tag{30}$$

- The electric displacement field is quasi-static for MT sounding periods. Therefore, time varying displacement currents (arising from polarization effects) are negligible compared with time-varying conduction currents; this promotes the treatment of electromagnetic induction in the earth purely as a diffusion process.
- Compared to bulk conductivity, all miniature variations of electrical permittivity and magnetic permeability are assumed to be negligible.

Both magnetic and electric fields are measured in orthogonal directions and are equated with the impedance tensor:

$$\begin{pmatrix} E_x \\ E_y \end{pmatrix} = \begin{pmatrix} Z_{xx} & Z_{xy} \\ Z_{yx} & Z_{yy} \end{pmatrix} \begin{pmatrix} H_x \\ H_y \end{pmatrix} \quad or \quad \boldsymbol{E = Z\,H} \tag{31}$$

$$E_x = Z_{xx}H_x + Z_{xy}H_y \tag{32}$$

$$E_y = Z_{yx}H_x + Z_{yy}H_y \tag{33}$$

Each $\boldsymbol{Z}$ component has both real and imaginary components.

For a 1D earth, conductivity varies only with depth and the diagonal elements of the impedance tensors, Z_{xx} and Z_{yy} (which couple parallel electric and magnetic field components) are zero, while the off-diagonal components (which couple orthogonal electric and magnetic field components) are equal in magnitude, but have opposite signs.

$$\left.\begin{matrix} Z_{xx} = Z_{yy} = 0 \\ Z_{xy} = -Z_{yx} \end{matrix}\right\} 1-D \tag{34}$$

In a homogeneous earth, all electromagnetic waves propagate vertically downward and the ratio of electric and magnetic field intensity is a characteristic property of the medium, also called characteristic impedance:

$$Z_{xy} = \frac{i\omega\mu_0}{k} = \frac{E_x}{H_y} = -\frac{E_y}{H_x} \tag{35}$$

where Z_{xy} = Characteristic impedance;
ω = Angular frequency;
μ_0 = Magnetic permeability in vacuum (Hm^{-1});
E_x, E_y = Electric field strength (Vm^{-1}) in x, y directions;
H_x , H_y = Magnetic field strength (Am^{-1}) in x, y directions;
k = $\sqrt{i\omega m_0(i\omega\varepsilon + \sigma)}$ is the wave propagation number;
ε = Dielectric permittivity (Fm^{-1});
σ = Electric conductivity (sm^{-1})

For a quasi-stationary approximation, $\sigma >> \omega\varepsilon$, the wave propagation number is approximated to $k = \sqrt{i\omega\mu_0\sigma}$ and impedance (Z) can be used to define apparent resistivity and phase:

$$\rho_{xy} = \frac{1}{\omega\mu_0}\left|Z_{xy}\right|^2 ;\ \theta_{xy} = arg\left(Z_{xy}\right) \tag{36}$$

$$\rho_{yx} = \frac{1}{\omega\mu_0}\left[Z_{yx}\right]^2 ;\ \theta_{yx} = arg\left(Z_{yx}\right) \tag{37}$$

Apparent resistivity calculated from off-diagonal elements of the impedance tensor for the 1D case, like in Equations 36 and 37, should be the same. But, in reality, the earth is never quite 1D, and we get two different resistivities in the *xy* and *yx* directions.

The apparent resistivity values and phases calculated from the tensor will, in general, depend on the orientation of the field layout. For 1D (layered earth) inversion, it is customary to use the determinant of the impedance tensor, which is rotationally invariant and provides a kind of an average value of the apparent resistivity. The determinant value is calculated as shown in Equation 38 and is used in 1D inversion:

$$\rho_{det} = \frac{1}{\omega\mu_0}|Z_{det}|^2 = \frac{1}{\omega\mu_0}\left|\sqrt{Z_{xx}Z_{yy} - Z_{xy}Z_{yx}}\right|^2 ;\ \theta_{det} = \arg(Z_{det}) \tag{38}$$

For a 2-dimentional (2D) earth, resistivity can vary with both depth and in one lateral direction, and the resistivity is constant in the other horizontal direction. The direction along which the resistivity is

constant is called the electric strike. If the field setup coordinate system is not parallel and perpendicular to the electrical strike, the MT impedance tensor data can be mathematically rotated with one axis perpendicular to the electrical strike and the other axis parallel to it, through minimizing the off diagonal elements of the impedance tensor. Thereby, we get Z_{xx} and Z_{yy} again equal to zero, like in the 1D case, but the difference is that, in 2D, $Z_{xy} \neq -Z_{yx}$. Sometimes it is not possible to find a strike direction that satisfies the condition $Z_{xx} = Z_{yy} = 0$, and that is because of 3D subsurface resistivity structure.

In the 2D case, magnetic and electric fields are considered as two independent modes. In transverse electric mode (TE mode), the electric field parallel to the electric strike depends only on magnetic field components perpendicular to the strike; in transverse magnetic mode (TM mode), the electric field perpendicular to the strike depends only on magnetic fields parallel to the electric strike.

In the 3D case, conductivity varies in all *x, y* and *z*, and all tensor elements are different. There is no rotational direction through which the two diagonal components of the impedance tensor become zero simultaneously.

Swift´s Skew is a normalized parameter used to describe the dimensionality of a resistivity structure:

$$skew = S = \frac{|Z_{xx} + Z_{yy}|}{|Z_{xy} - Z_{yx}|} \tag{39}$$

If the value of S is large, it means that we are dealing with a 3D earth, but if we get a small value (for example 0.2), it means that we are working in a 1D or 2D earth.

For an N-layered earth, the impedance at the surface, $\hat{Z}_o$, can be calculated recursively. Impedance for n^{th} layer is defined as (Ward and Wannamaker, 1983):

$$\hat{Z}_N = \frac{\omega\mu_0}{k_N}\ ; \hat{Z}_n = Z_n \frac{\hat{Z}_{n+1} + Z_n tanh(ik_{n-1}h_{n-1})}{Z_n + \hat{Z}_{n+1} tanh(ik_{n-1}h_{n-1})} \tag{40}$$

where $Z_n = \frac{\omega\mu_0}{k_N}$ = The intrinsic impedance of the n^{th} layer;

$k_N = \sqrt{(i\omega\mu_0\sigma_n)}$

h_n = thickness of the n^{th} layer;

$\hat{Z}_n$ = Impedance of the n^{th} layer.

For a simple two-layered system:

$$\hat{Z}_1 = Z_1 \frac{\hat{Z}_2 + Z_1 tanh(ik_1h_1)}{Z_1 + \hat{Z}_2 tanh(ik_1h_1)} \tag{41}$$

where $\hat{Z}_1 = \hat{Z}_o$ = the impedance at the surface; and

$k = \sqrt{\frac{\omega\mu_0}{\rho_1}} = \sqrt{\frac{2\pi\mu_0}{\rho_1 T}}$

3.2.1 Static shift problem

The MT method monitors and measures electric field variations in the subsurface. Due to discontinuities in underlying layers, electric and magnetic fields can be distorted. Multi-dimensional conductivity contrasts lead to incorrect depth estimates, called 'static shift'. This static shift is called "static" because the conservation of current at conductivity discontinuities is not a time-dependent process like, for example, induction. Therefore, the phenomenon of static shift does not affect the phase of the transfer function (Simpson and Bahr, 2005). There are two mains reasons for MT static shift, aside from topographic distortion:

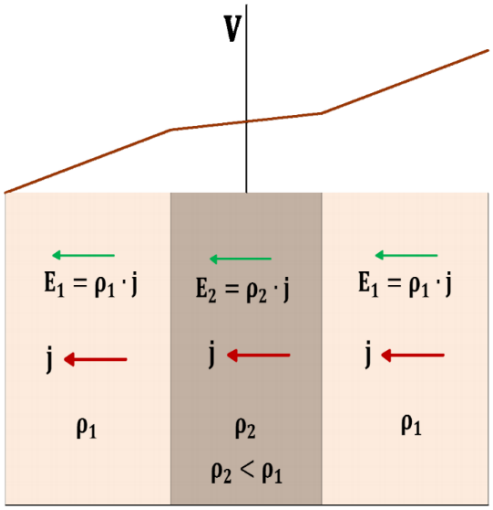

FIGURE13: Electric field distortion (Sternberg et al., 1988; Árnason, 2008)

Electric field distortion: In this case due to the vertical resistivity discontinuity, the electric field (voltage difference over a given length) is lower in the low-resistivity domain. Conductivity discontinuities like the ones shown in Figure 13 cause local distortion of the amplitudes of electric fields as a result of conservation of electric current, hence causing impedance magnitudes to be enhanced or diminished by real scaling factors.

Current distortion (current channelling/ repelling): Superficial bodies can severely and arbitrarily distort the current distribution. This will distort the electric field and cause the impedance magnitude to increase or decrease by a real scaling factor and therefore shift the apparent resistivity curve up or down on the log scale. For example, in Figure 14 the superficial body with resistivity, ρ_2 is channelling the current because its resistivity is lower than the rest of the subsurface with resistivity, ρ_1. But if this body had a resistivity higher than ρ_1, the current would be repelled by the body.

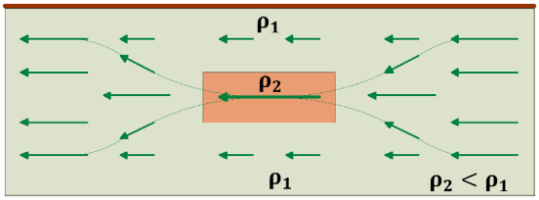

FIGURE 14: Current distortion (Sternberg et al., 1988; Árnason, 2008)

4. ELECTROMAGNETIC DATA ACQUISITION SYSTEMS AND ANALYSIS

In order to gather good data, we need to follow certain field procedures. Most of them are intended to prevent or reduce user errors, instrumental errors and other possible ambiguities. Before field measurements are taken, field crews must be concerned with field conditions and possible electromagnetic noise sources. Any disturbances which can affect data quality must be avoided. Possible noise sources can include:

- Electric fences,
- Moving vehicles,
- Electricity transmission lines,
- Electric pumps,
- Mechanical vibration sources.

Though the topography of a sounding site is not a major concern, it is better to have a plane area to establish an MT sounding site.

4.1 TEM data acquisition

Geonic's Protem instrument system was used for data acquisition. The following instrument modules are needed for measurements at a TEM sounding site:

- Generator (240 V /5 kva) /and or battery bank (100 V),
- Transmitter (TEM 57 MK 2),
- Power booster (TEM 87),
- Transmitter loop-1200m (300 m × 300 m loop),

- Receiver (Protem),
- Receiver coils (effective area; 100 m^2, 5613 m^2),
- Reference cable,
- GPS,
- Clinometer.

Synchronization is necessary between the receiver end and the transmitter end. There are two methods available for synchronization. Use of a reference cable or a crystal clock is very common. But in modern instruments, satellite (GPS clock) synchronization is also available. All crystals (quartz) in both receiver and transmitter must be heated to standard temperature and this temperature should be maintained for the assessing period.

Basic dimensions of the transmitter loop depend on the depth of penetration which is intended. In this field work, a single turn 300 m × 300 m transmitter loop was laid. The receiving loop was placed in the middle of the transmitting loop. There is a choice of two receiving loops, which have different effective areas. After the basic preparations, current was injected in a low frequency mode and turn off time (T_{off}) was determined in the transmitter.

Before making any measurements, the receiver (Protem) is calibrated and receiver coil parameters need to be recorded in the instrument log. Appropriate gain is required for meaningful data acquisition. After basic setup in the receiver, a half duty square wave current was transmitted at frequencies 25 and 2.5 Hz. The transient signal was recorded in the different time intervals logarithmically spaced sampling gates after the current turn-off. For each frequency, several repeated transients were stacked and stored in a memory inside the Protem receiver.

4.2 MT data acquisition

There are several ways to set up an MT sounding site (Figure 15). Though the site preparation is easier than for TEM, there are some rules that need to be addressed for successful sounding points:

- Avoid root systems from nearby trees;
- Anchor connecting cables;
- Self-potential of ground should be < 25 mv;
- Grounding procedures.

General components needed for an MT sounding point:

1. Recording unit;
2. Power source (12V battery);
3. GPS receiver;
4. Induction coils (3);
5. Non-polarizing electrodes (5);
6. Augur tool and other excavating tools;
7. Bubble level;
8. Ranging poles;
9. Clinometer;
10. Plastic bags.

A nearly planar area (50 m × 50 m) is favourable for an MT sounding site. Electrodes must be placed in both north-south and east-west directions with at least 50 m separation. All electrodes including earth electrodes need to be buried at least 30 cm underground and ground contact should be good. Some salt water is poured into the base hole and some bentonite clay is placed around the electrode.

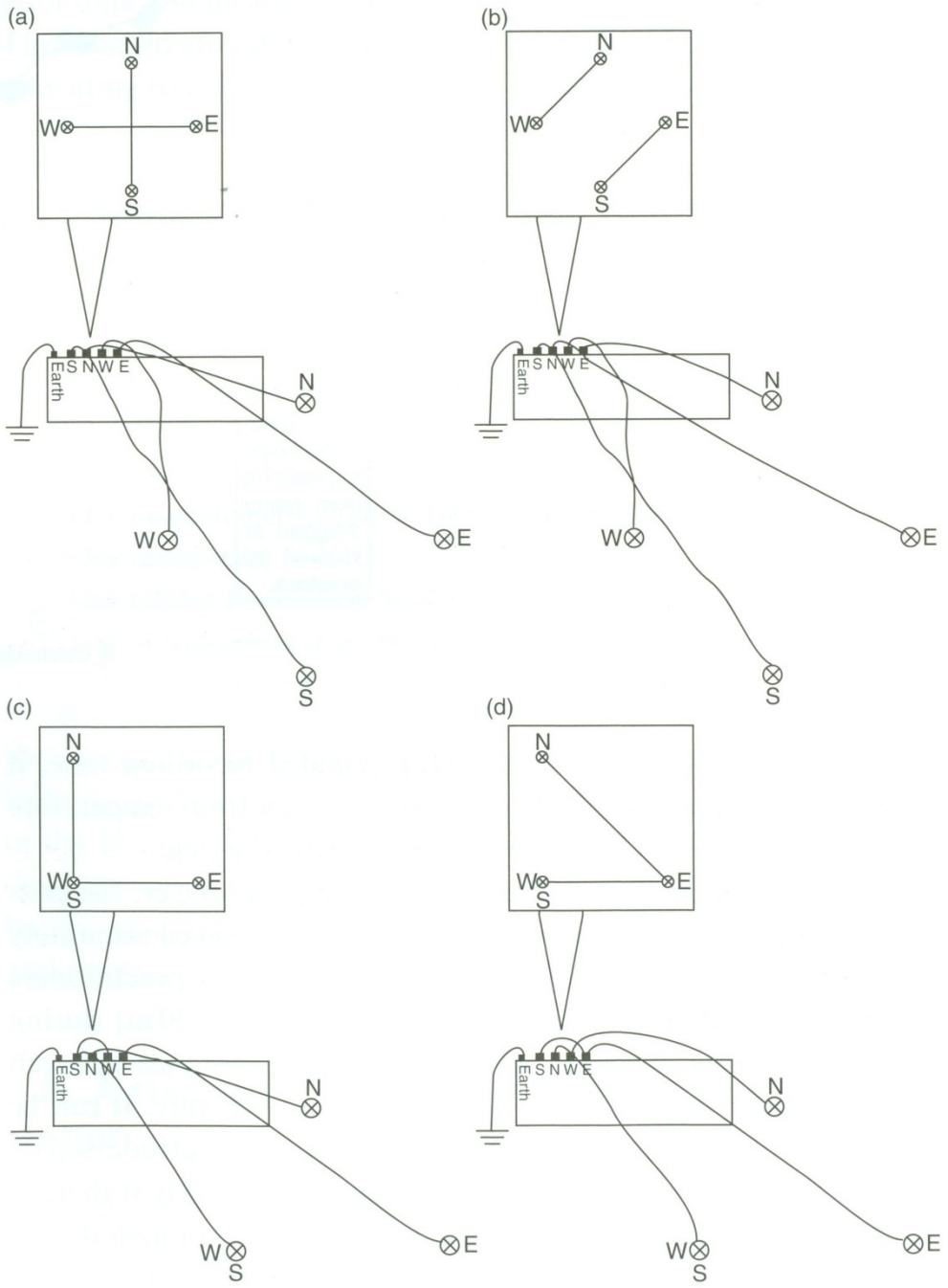

FIGURE 15: Different MT sounding site configurations
(Simpson and Bahr 2005)

Magnetometers must be laid in north-south and east-west directions precisely and should be levelled using a bubble level. To assure proper alignment and levelling, all magnetometers should be buried at around 25 m from the recording unit. Coaxial cables are used to connect electrodes to the recording unit and the outer shield of the co-axial cable should also be grounded. Movement of cables can generate electromagnetic noise. Therefore, all connecting cables must be anchored properly.

After connecting all magnetometer coils, electrodes and GPS receiver, and the memory card containing the start-up program, the recording unit is turned on. After this, the recording unit can be left for data collection. Collected data can be downloaded with a portable computer. Preferably, the quality of each MT sounding point is assessed on-site to see if it is necessary to replicate the reading.

4.3 Application/processing and inversion of TEM and MT data

In this study 15 TEM and MT soundings from sites in Theistareykir area were processed. Figure 16 shows their locations. The majority of them were collected by ÍSOR between the years 2009 and 2011; with one MT sounding site being repeated in 2012. The raw data from TEM and MT time series were processed during this project period. The results of the 15 MT soundings and data processing are given in Appendices published separately in a special report (Suriyaarachchi, 2012).

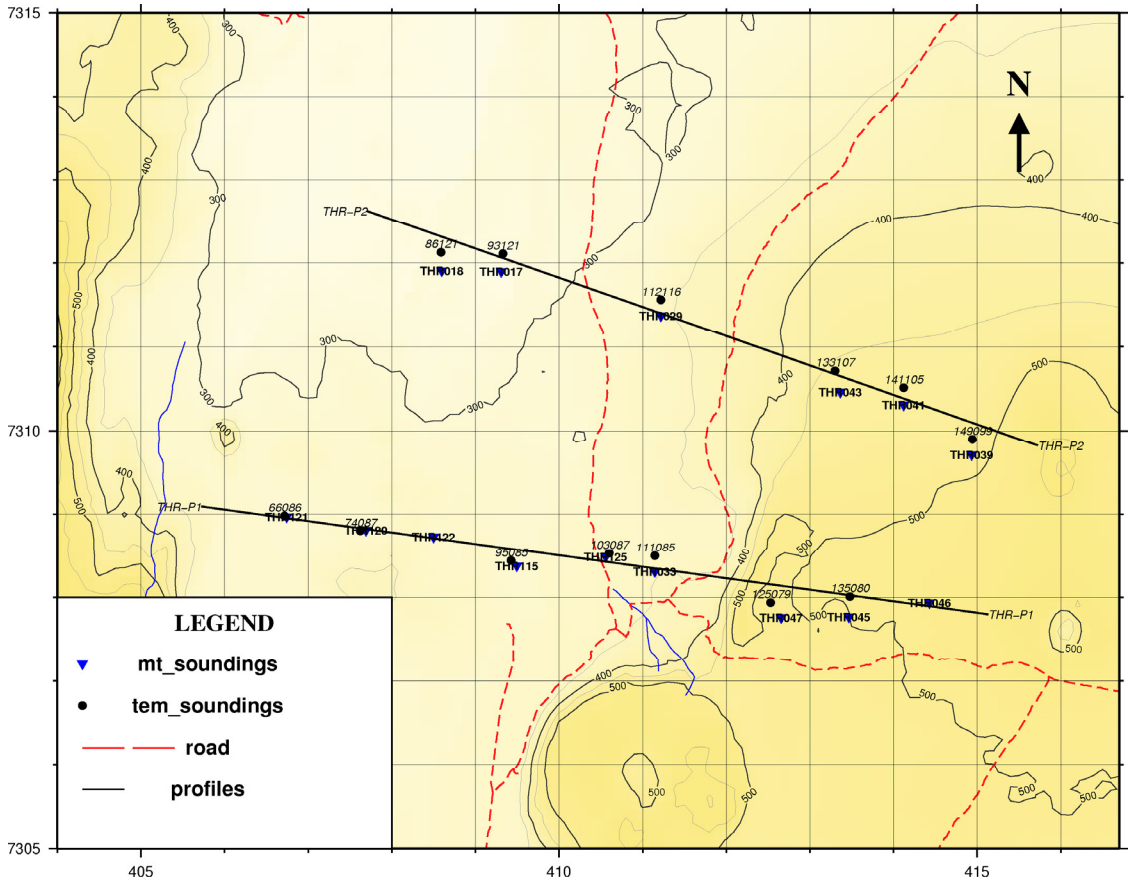

FIGURE 16: Theistareykir, location of the 16 measuring sites and the resistivity profiles P1 and P2

4.3.1 TEM data processing

TEM data processing is the first step in processing the data. The program TemX (Árnason, 2006a) was used to import data from the raw data files. It was also able to throw out some disturbed data points, by considering different frequency bands, and the best penetration depths. The TemX programme calculates the averages and standard deviations of the repeated transient voltage measurements and computes apparent resistivity as a function of time. This program also provides a graphical interface to reject outlier data points by just clicking on them; a restoration ability is accomplished with a right click on deleted data points. Inversion of TEM data is the next phase. The TEMTD program (Árnason, 2006b) was used for both TEM and MT data interpretation. This program was developed by ÍSOR's geophysical staff and is used to perform 1D layered-earth inversion of resistivity data. The current waveform is also assumed to have equal current-on and current-off time segments. The transient response is calculated both as induced voltage and late time apparent resistivity as a function of time.

TEMTD also offers a wide range of options for better 1D data inversion. A basic model is fed into the program. This model, also called the initial model, nearly correlates to the resistivity curve from TemX. The initial model may consist of 4-7 resistivity layers. This initial model does not necessarily have to be precise or correct. But a reasonable initial model can save a lot of computer time.

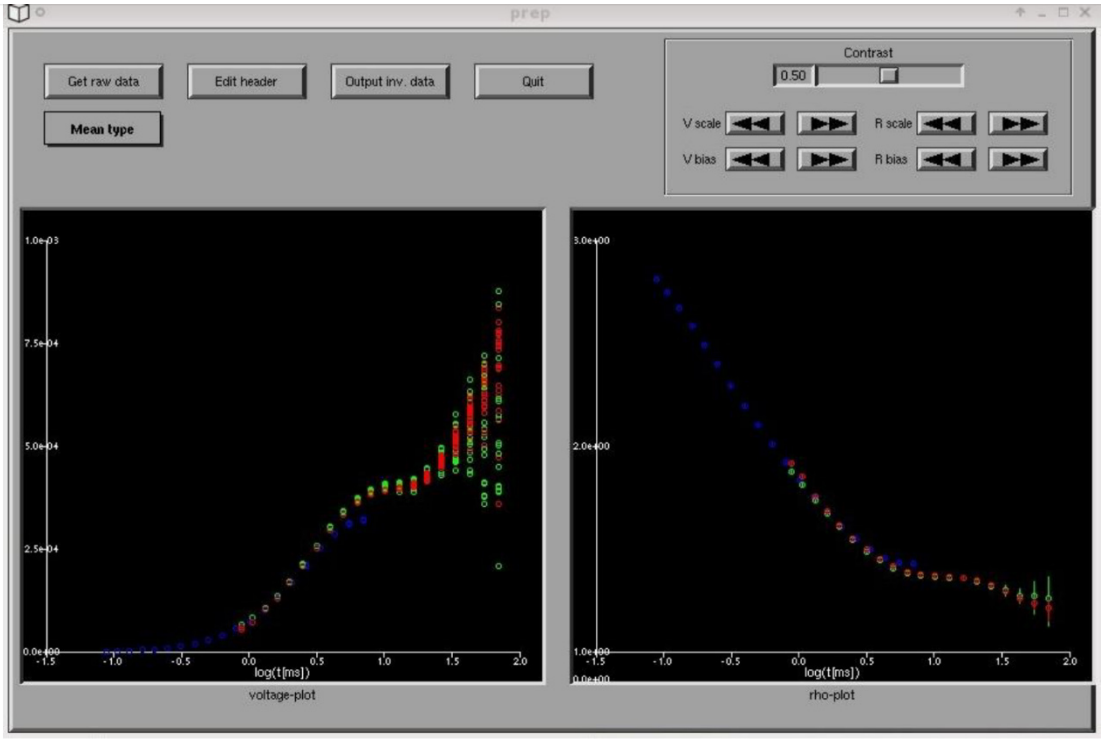

FIGURE 17: TEMX user interface

The TEMTD program is run on a Linux/Unix operating system platform (Figure 17). The inversion algorithm used in the program is the nonlinear least-squares inversion of the Levenberg-Marquardt type (Árnason, 1989). The misfit function is the root-mean-square difference between measured and calculated values (chisq), weighted by the standard deviation of the measured values. The user is offered the option of choosing whether the program fits the measured voltage or the late time apparent resistivity values.

The program offers the possibility of keeping models smooth, both with respect to resistivity variations between layers (logarithm of conductivities) and layer thickness (logarithm of ratio of depth to top and bottom of layers). The damping can be done both on the first derivatives, which counteract sharp steps in the model, and on the second derivatives, which counteract oscillations in the model's values. The actual function that is minimized is not just the weighted root-mean-square misfit, 'chisq', but the 'potential':

$$Pot = chisq + \alpha\, DS1 + \beta\, DS2 + \gamma\, DD1 + \delta\, DD2 \qquad (42)$$

where *DS1, DS2* = First and second order derivatives of log-conductivities in the layered model;
DD1, DD2 = First and second order derivatives of logarithms of the ratios of layer depths;
$\alpha, \beta, \gamma, \delta$ = Coefficients that are the relative contributions of the different damping terms.

TEMTD is also used to perform minimum stricture (Occam´s) inversions. In an Occam inversion, layer thicknesses are kept fixed (Figure 18), equally spaced on a log scale, and the conductivity distribution is forced to be smooth by adjusting α and β (Equation 42).

4.3.2 MT data processing

The SSMT2000 program was used to handle MT time series data. This program was provided by the equipment manufacturer, Phoenix Geophysics of Canada. First the parameter files were edited to reflect the data acquisition setup and then the resulting time-series data were Fourier transformed to the

frequency domain. From the Fourier transforms band, averaged cross and auto powers were calculated using the robust processing method.

In order to improve the smoothness of the apparent resistivity and phase curves, the MT-Editor program was used to remove noisy data points. All relevant MT parameters were calculated from them such as impedances, apparent resistivity, phase coherences, strike directions, etc., exported as EDI files ready for joint inversion by TEMTD.

5. RESISTIVITY DATA FROM THEISTAREYKIR

5.1 Geological setting of Theistareykir high-temperature geothermal area

Theistareykir is a high-temperature geothermal field in NE-Iceland. The main features in the geology of the area are an E-W trending heat source astride a N-S tectonic structure connected to an active central volcano. A fissure swarm, 4-5 km wide, stretches from Lake Mývatn in the south to the sea in Öxarfjördur in the north. The whole area is covered with lava and the youngest lava is around 2700 years old. Though surface manifestations spread over around 11 km^2, recent TEM and MT surveys showed that the actual geothermal field could be spread over 40 km^2.

The regional geology has been described in detail by Saemundsson (2007), who added to, and expanded on, the work of Torfason (Gíslason et al., 1984). The local geology is summarized in Figure 19. A red line encompasses the high-resistivity core at around 1 km depth. It looks like it marks the edge of alteration associated with the geothermal system. The oldest hyaloclastites, Lambafjöll, are

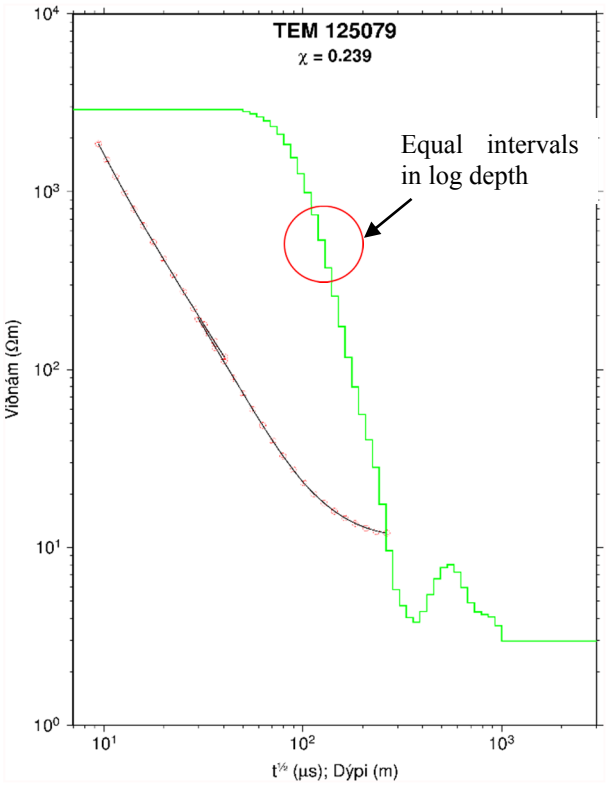

FIGURE18: Inversion of TEM data

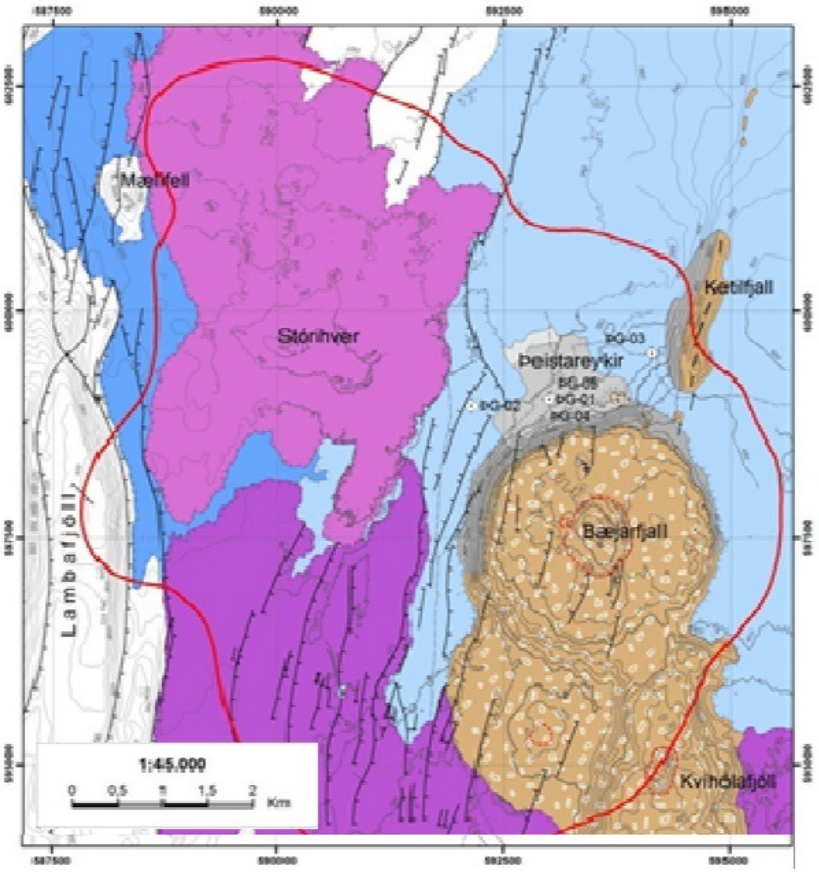

FIGURE 19: Geological map of the Theistareykir area (Saemundsson, 2007)

not coloured; the younger hyaloclastites are coloured brown. Younger lava flows in blue and purple include Theistareykjahraun which is light purple in colour.

Ketilfjall is the oldest hyaloclastite formation, close to the geothermal centre at Theistareykir. It formed in a fissure eruption underneath the Quaternary ice-sheet on a 4 km long fissure. Baejarfjall and Kvíhólafjöll are younger tuyas, or table mountains, formed by eruptions on short fissures or single volcanic vents.

The highland between the hyaloclastite mounds and ridges is covered by basaltic lava-flows. The flows in the area are very old; only one of the flows is considered to be less than 10,000 years old. This is Theistareykjahraun, which is considered to be around 2500 years old (Saemundsson, 2007). The lava flows have partially buried the sub-glacial table mountains and ridges so their "roots" are hidden.

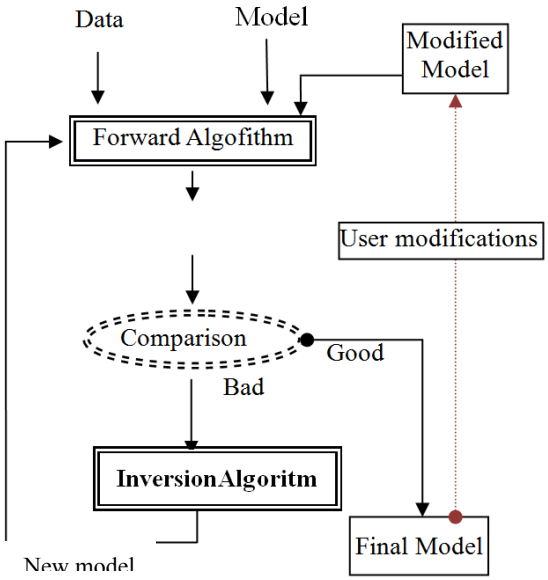

FIGURE 20: Flow chart for joint inversion

5.2 1D joint inversion of TEM and MT data

Both TEM and MT resistivity data need to be successfully inverted, a process, called joint inversion. The program called TEMTD is used for this with appropriate options and parameters. According to the initial model that is given to the program, TEMTD produces a model. Then it compares differences and calculates again for a reasonable fit for the calculated model. This is called an iteration process. Figure 20 shows a general block diagram for the joint inversion process.

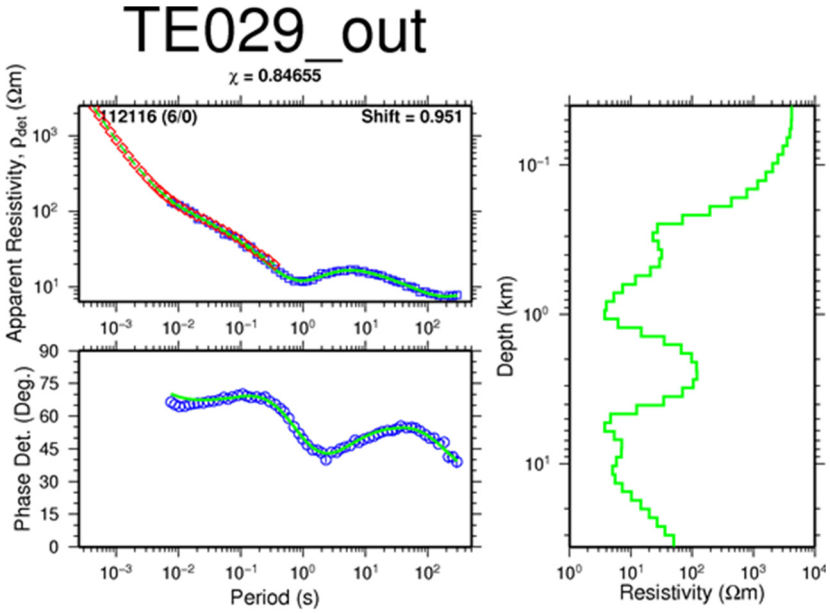

FIGURE 21: Combined resistivity, phase graphs from joint inversion

In the TEMTD program, both TEM and MT resistivity curves were combined together, in order to obtain the best fit. Figure 21 shows the combined apparent resistivity from MT, TEM and phase response in the right panel, resulting from the 1D resistivity inversion model. For this data inversion, MT and TEM data had to be recorded on relatively the same dates and in the same place. The title on the top of the figure (TE029_out) is the name of the MT sounding site which was used. The number in the upper left corner of Figure 21, (6 / 0), describes the distance and difference in elevation of the MT and TEM sounding points. A shift multiplier (shift = 0.951) also appears in the same panel, stating the shift between the MT and TEM apparent resistivity curves.

The TEMTD program gave (TE029).out and (TE029_112116).plo files as its outputs for this particular 1D inversion. The (TE029).out file contained output data from MT and the (TE029_112116).plo file contained the final model calculated from the MT and TEM data. Those files needed to be processed with TEMCROSS (Eysteinsson, 1998) in order to create resistivity cross-section profiles. The program called TEMRESD (Eysteinsson, 1998) was used to create iso-resistivity maps for interesting depths.

5.3 Static shift for in the Theistareykir area

Due to local resistivity inhomogeneities, electric fields can be distorted. This phenomenon is called static shift. For instance, a shift down by S = 0.1 will, in interpretation, result in ten times too low resistivity values and about three times too small depths to resistivity boundaries (Árnason, 2008). There are few advanced methods available to minimize static shift. DeGroot-Hedlin (1991) and Ogawa and Ushida (1996) proposed the use of an inversion algorithm on MT data to correct for static shift; this assumes that the shift multipliers are random and that the product of the shift multipliers is close to one for many soundings. This may not necessarily be correct.

The use of central loop-induction TEM soundings to correct for static shift in MT data by jointly inverting both MT and TEM data is another method. This method is based on the fact that for TEM measurements at late time there are no distortions due to near surface inhomogeneities since they do not involve measuring the electrical field. This has been tested by model calculations (e.g. Sternberg et al., 1988) and shown to be a useful method for correcting for static shifts in MT soundings.

The shift distribution for the studied area is shown in Figure 22 and its values are distributed around 0.8 (Figure 23). The TEM apparent resistivity used to estimate the shift parameter in the MT data does not necessarily agree with the principle apparent resistivity of Z_{xy} or Z_{yx}. It may occur between them, below them or agree with either of them. It should also be noted that the phase is not affected by the static shift problem.

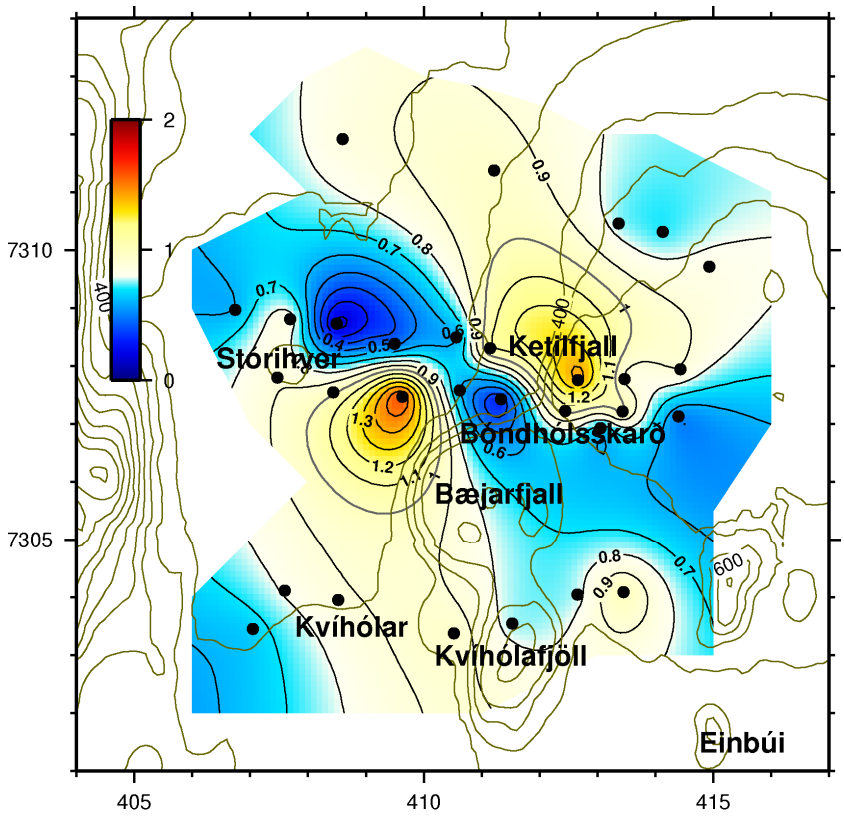

FIGURE 22: The static shift distribution over the studied area

5.4 Strike directions

The electrical strike direction says there is a 2D resistivity structure in the underlying layers. The direction of least resistivity changes present can be found through tensor analysis. Electrical strike direction can be calculated by minimizing the diagonal elements of the impedance tensor components denoted from Z_{xx} and Z_{yy}. Even after the intense calculations, there is a 90° ambiguity in the electric strike (Z-strike analysis). In order to minimize this ambiguity, H_z, the horizontal magnetic component needs to be measured. This is also called the tipper direction (T-strike analysis) analysis. Most of the time, strike direction agrees with subsurface distribution, simultaneously giving information about the flow paths of the geothermal fluid in relation to permeability.

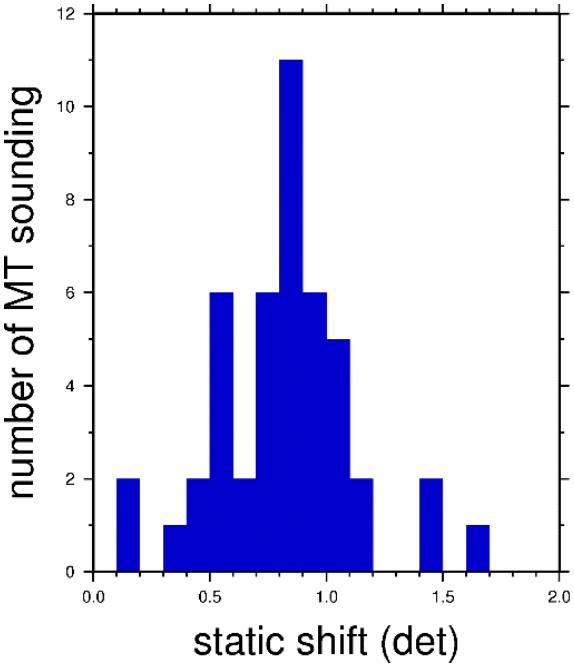

FIGURE 23: Static shift histogram

It is possible to have different tipper directions for different time periods. Different times stand for different depths. Generally, resistivity data from the 0.01 to 1vs (Figures 24 and, 25) period can represent up to 1 km, while the 1 to 100 s period (Figures 26 and 27) data represent up to several tens of kilometres. This gives us an idea of the main variations in conductivity direction at different depths.

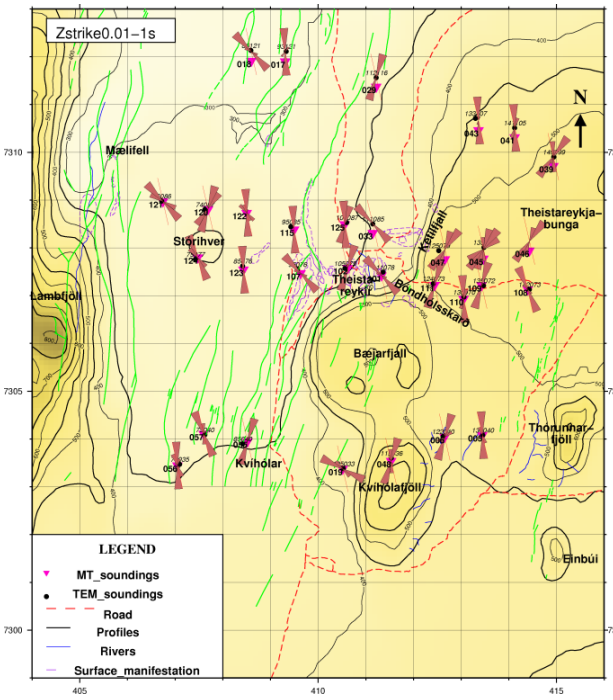

FIGURE 24: Z-strike for 0.01 - 1.0 s interval

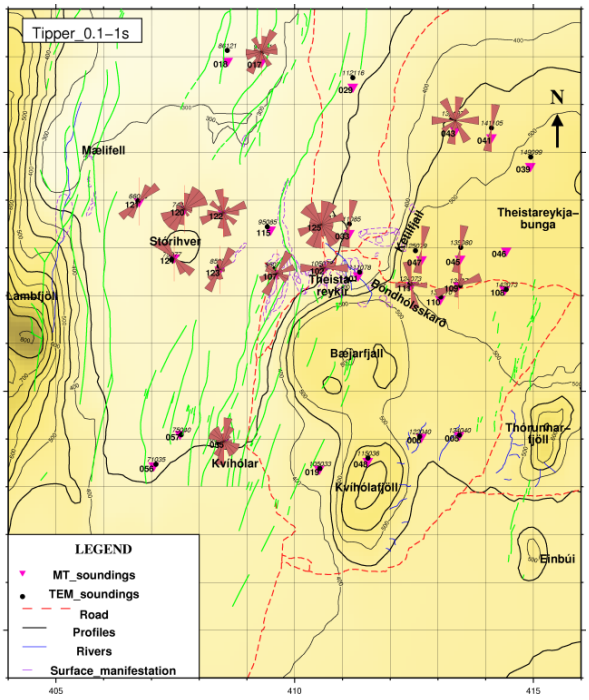

FIGURE 25: T-strike for 0.01 - 1.0 s interval

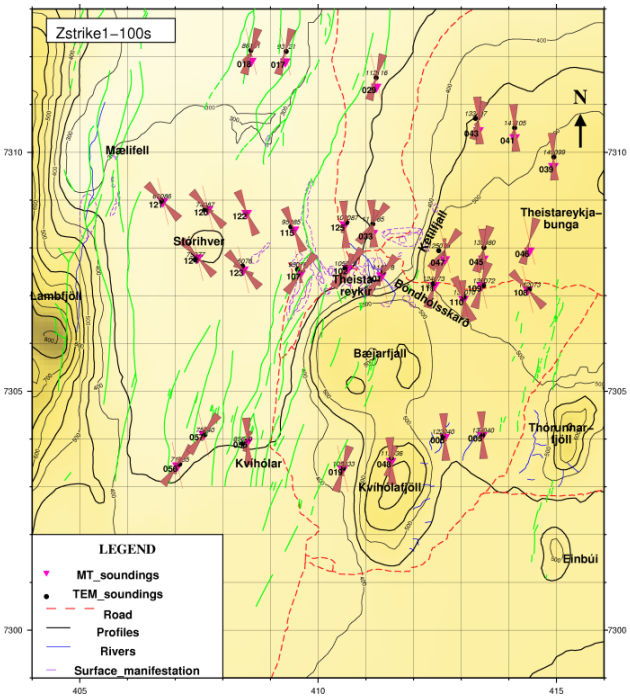

FIGURE 26: Z-strike for 1 - 100 s interval

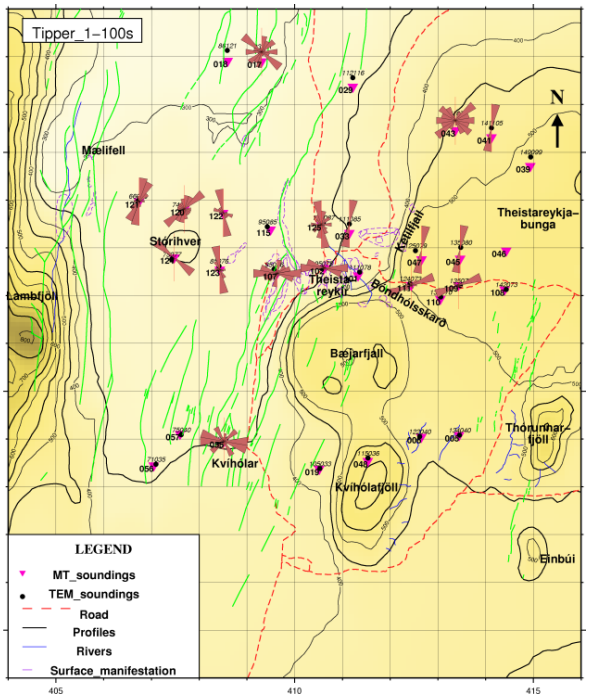

FIGURE 27: T-strike for 1 - 100 s interval

5.5 Resistivity cross-sections and results from boreholes

Combining all resistivity models, two resistivity cross-sections were made. Both joint inversion results and TEM resistivity models were used to make these cross-sections. As mentioned earlier, the resistivity structure of a high-temperature system reflects the thermal alteration of the rocks. A low-resistivity cap refers to the smectite-zeolite zone with high conductivity. The underlying high-resistivity core refers to the chlorite-epidote zone with temperatures exceeding 250°C. If there is equilibrium between the temperature in the system and the alteration, the resistivity structure will reflect the temperature in the geothermal system. If there is cooling in the system, the alteration may reflect the formation temperature rather than the existing temperature. Thus, the alteration will always show the maximum temperature that has prevailed in the system. The actual temperature in any system can only be verified by drilling.

A characteristic resistivity structure of a high-temperature system is a low-resistivity cap underlain by a high-resistivity core. High resistivity above and around the low-resistivity cap is due to unaltered rock at the surface. A low-resistivity body at greater depths may indicate the heat source of the geothermal system.

The results of the joint inversion of TEM and MT soundings are presented as resistivity cross-sections P1 and P2, as well as iso-resistivity maps for the available resistivity data. Figure 28 shows resistivity cross-section P1 down to 5 km depth b.s.l. A highly resistive unaltered upper layer is present at the surface and this layer can also be seen clearly in the TEM resistivity cross-section (Figure 29). In the next layer, low-resistivity alteration minerals become dominant. Beyond that a highly resistive core is clearly indicated, thinned down by another low-resistive body which extends beyond 5 km.

Figures 30 and 31 give similar results for resistivity profile P2, located 2-3 km north of P1. The upper margin of the low-resistivity cap is at a greater depth (200 m b.s.l.) than in P1 and extends about a 1 km down. Then the highly resistive core appears, about 2 km thick, and a low-resistivity deep layer lies beyond 5 km depth. The TEM resistivity cross-section for profile P2 shows a highly resistive surface layer (unaltered) and two other altered layers with a clear boundary.

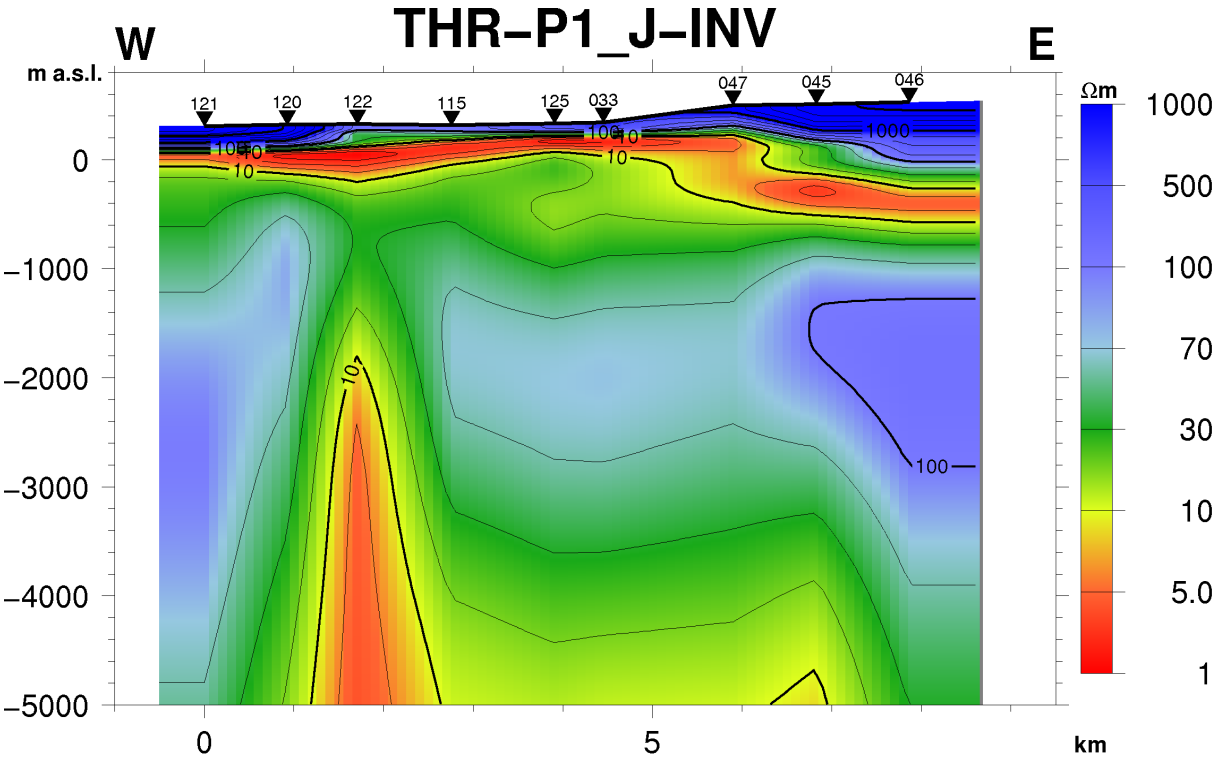

FIGURE 28: Resistivity cross-section from profile P1 trending W-E, based on joint inversion

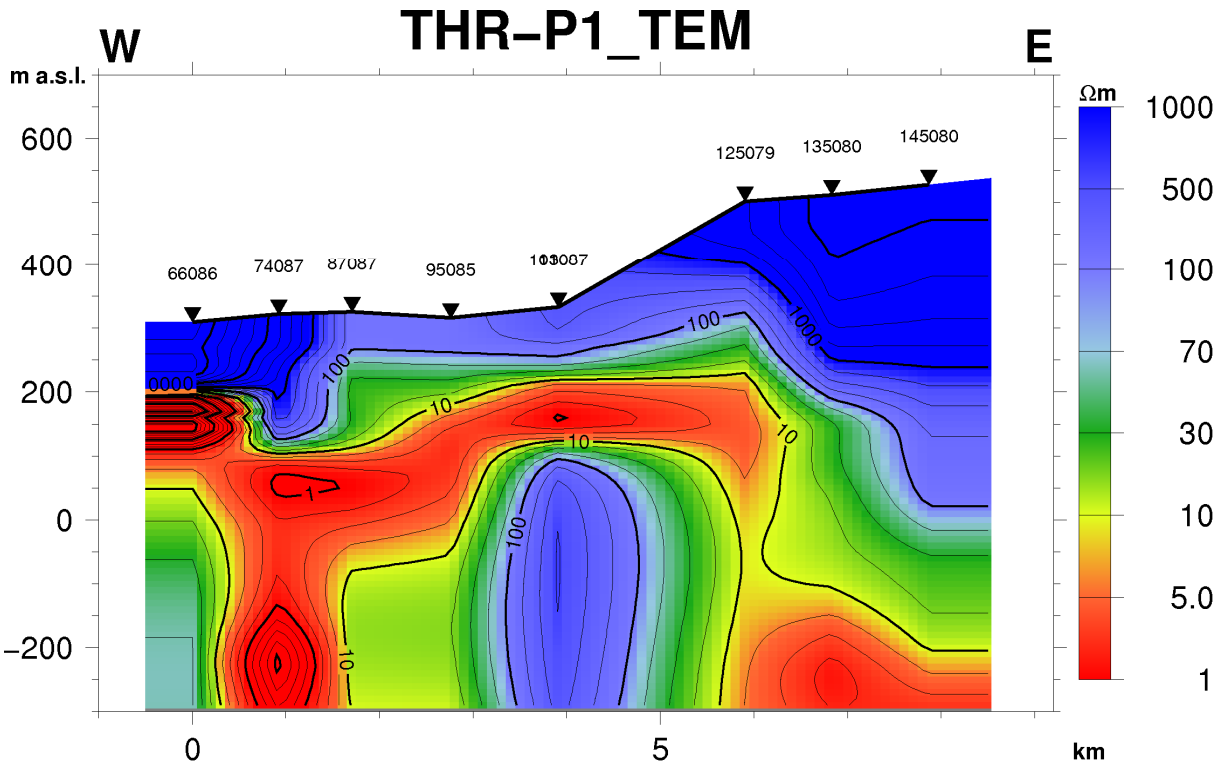

FIGURE 29: Resistivity cross-section from profile P1, trending W-E, based on TEM

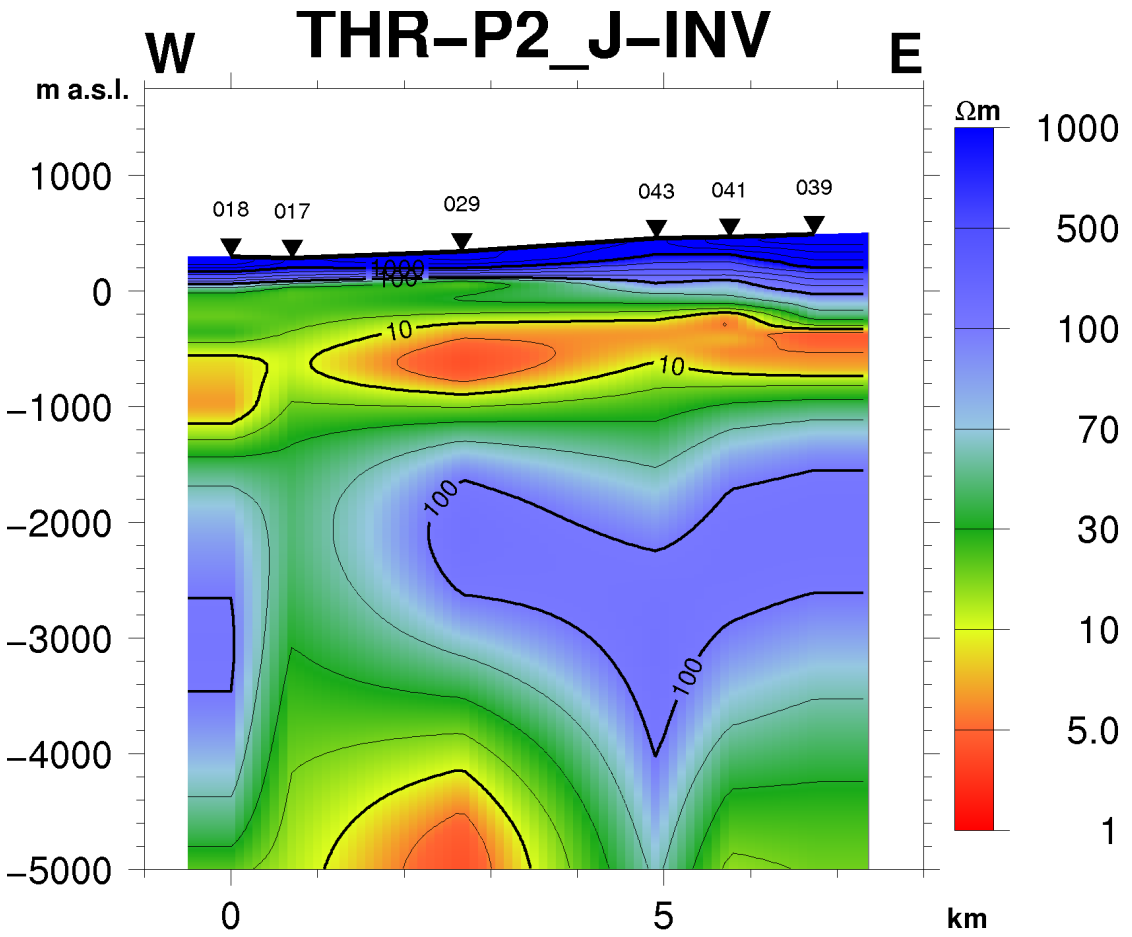

FIGURE 30: Resistivity cross-section from profile P2, trending WNW-ESE from joint inversion

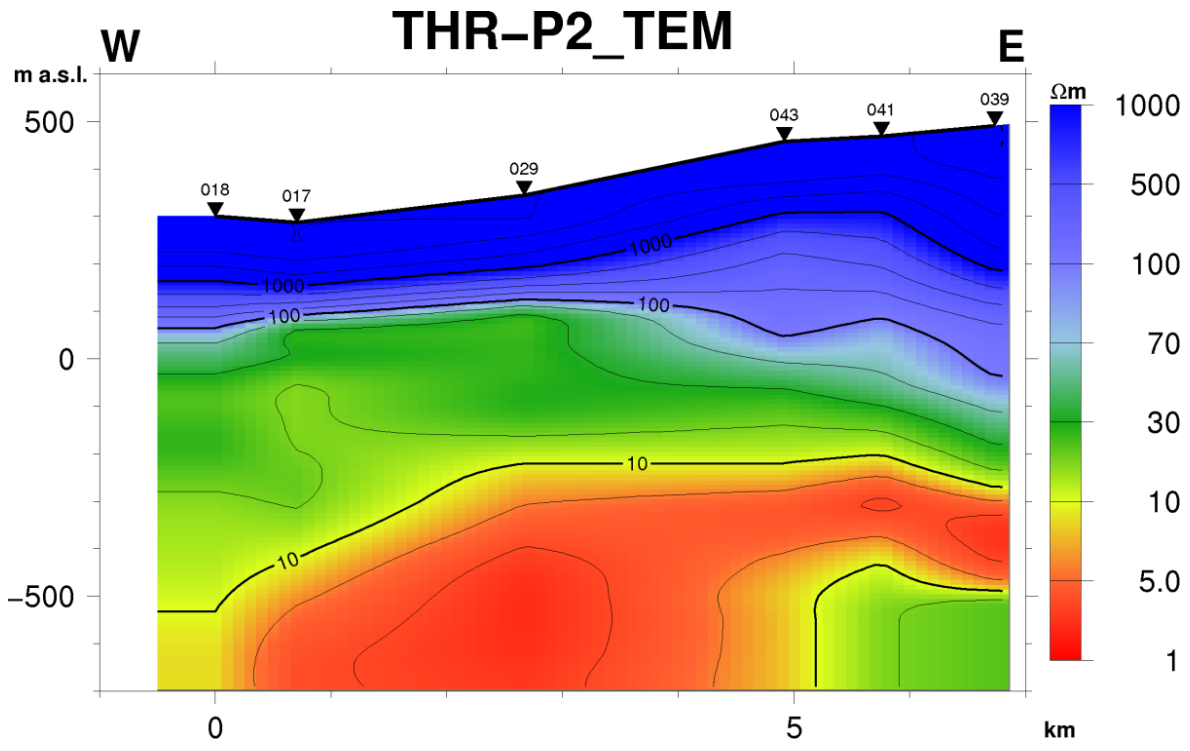

FIGURE 31: Resistivity cross-section from profile P2, trending WNW-ESE based on TEM

5.6 Resistivity maps

There are different methods used to represent resistivity data. Iso-resistivity maps clearly address horizontal resistivity variations. Figures 32-35 show iso-resistivity maps for different depths. Here, additional data from UNU Fellow, E. Kahwa (2012) were also used to give more clarity to the maps. Figure 32 shows the unaltered rocks (> 100 Ωm) close to the surface and the low-resistivity cap (< 5 Ωm) emerging at Theistareykir and Bóndhólsskard. The map at sea level (Figure 33) shows the lowering resistivity at the upper margin of the low-resistivity cap and the two tops of the low-resistivity cap, one at Bóndhólsskard and another north of Stórihver. Figure 34 shows resistivity within the high-resistivity core at 1000 m b.s.l. Figure 35 shows resistivity at 10 km depth b.s.l. and reveals a deep seated low-resistivity body that may indicate the heat source of the geothermal system.

For better understanding of the resistivity structure, the results of profile P1 were compared with the alteration mineral data from a nearby borehole. Though the borehole is located 600 m away from profile P1, the alteration mineral sequence is a fair match. The conductive zeolite and smectite zone appears within the low-resistivity cap and the more resistive chlorite/epidote appears within the high-resistivity core.

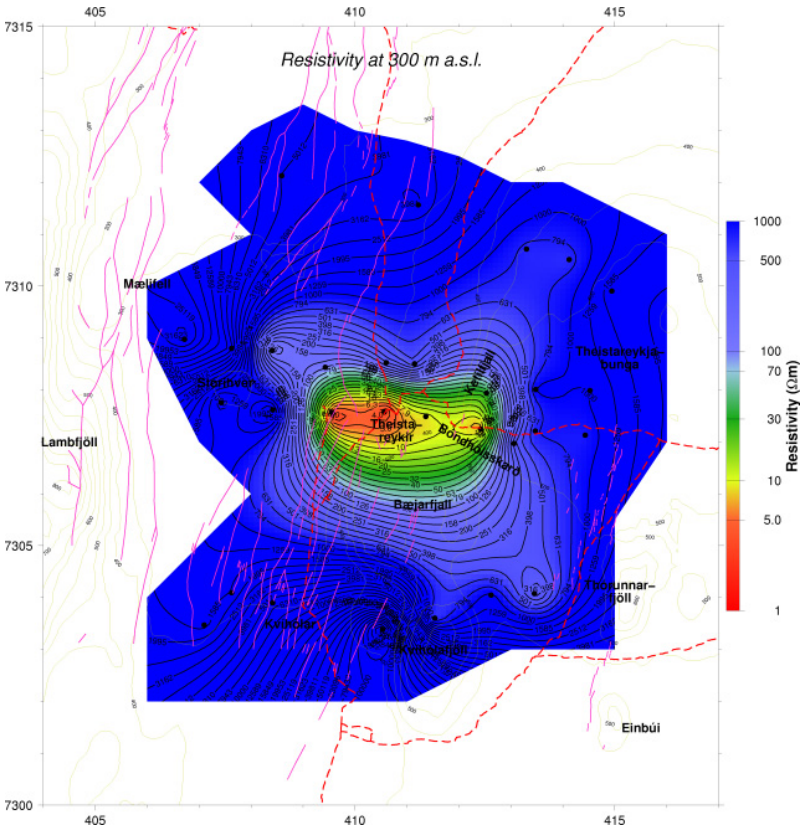

FIGURE 32: Theistareykir field, iso-resistivity map at 300 m above sea level

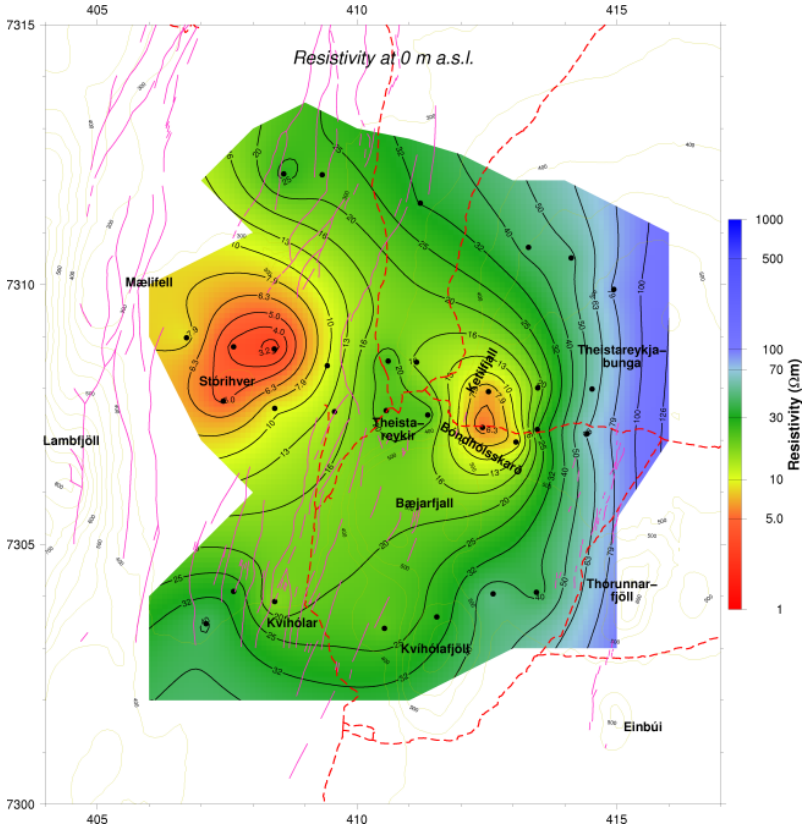

FIGURE 33: Theistareykir field, iso-resistivity map at sea level

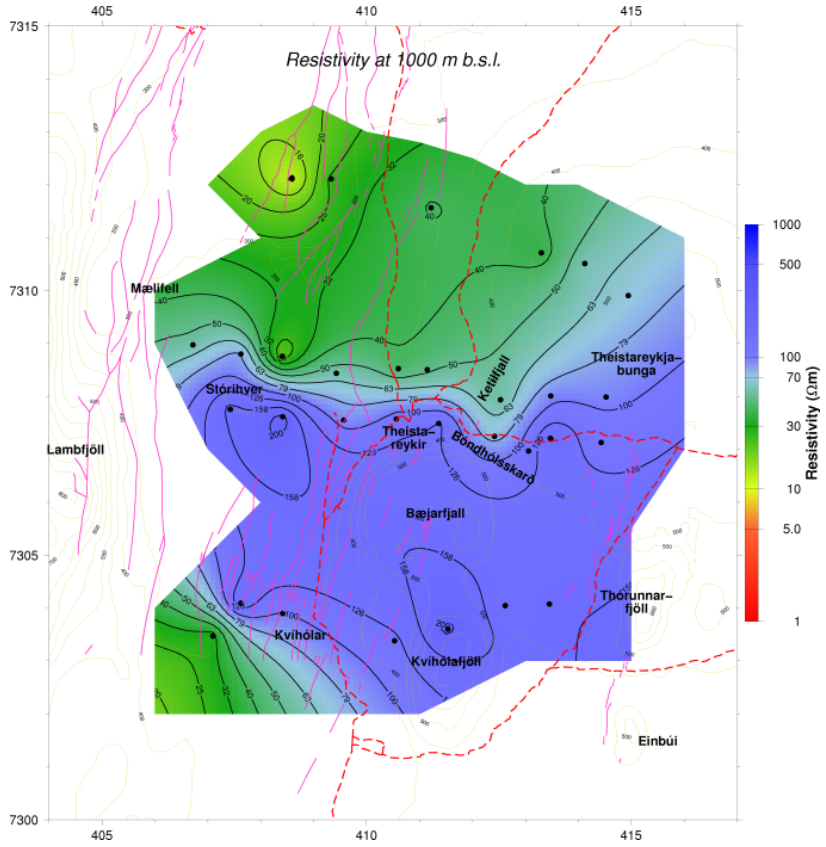

FIGURE 34: Theistareykir field, iso-resistivity map at 1000 m below sea level

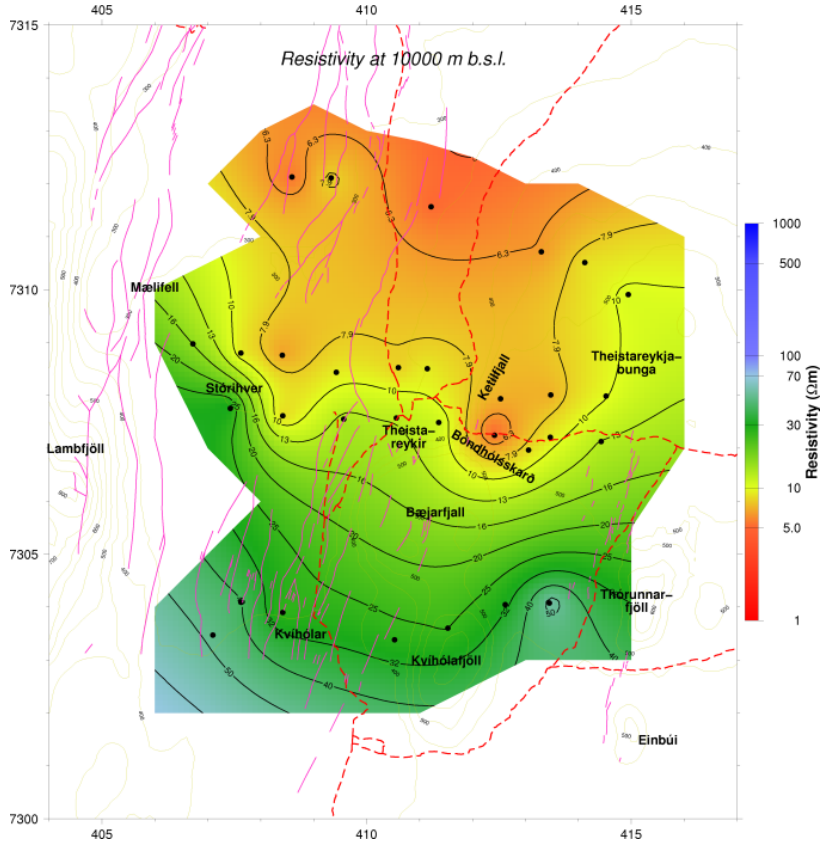

FIGURE 35: Theistareykir field, iso-resistivity map at 10,000 m below sea level

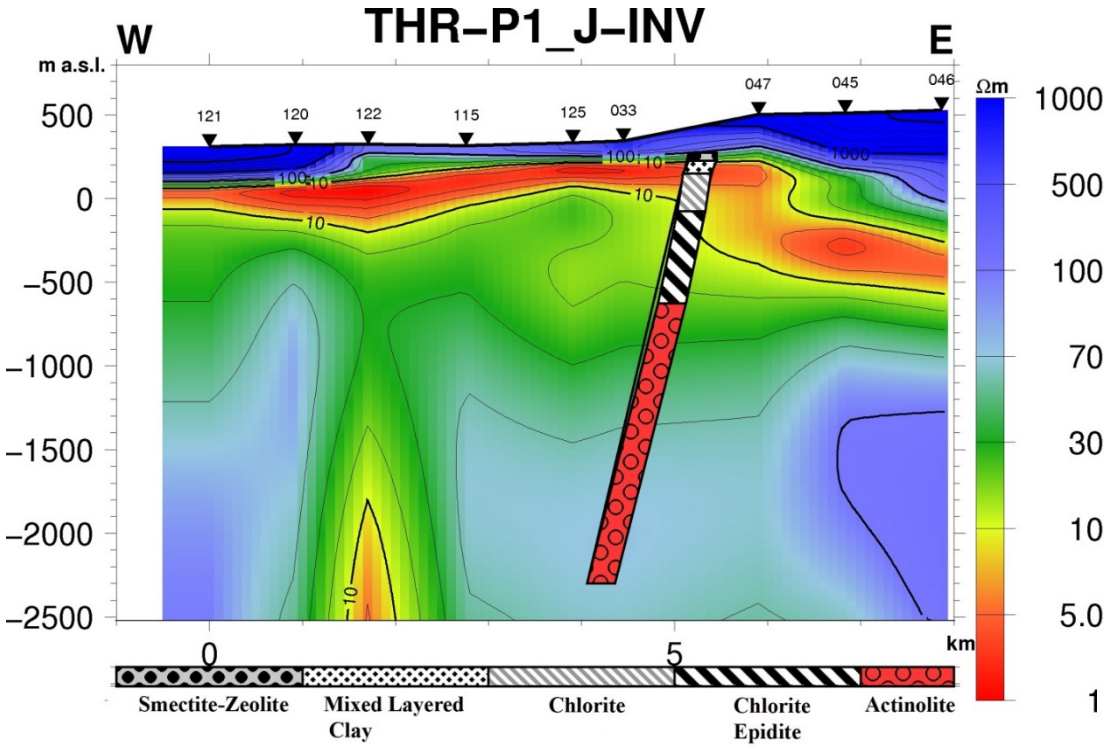

FIGURE 36: Resistivity structure of profile P1 compared with the mineralogy from a well

6. DISCUSSION AND CONCLUSIONS

- Combining TEM and MT is an effective and promising method for geothermal resource exploration. Properly spaced electromagnetic soundings can be used for interpreting both vertical and horizontal resistivity contrasts.
- Near surface resistivity variations can cause false interpretations. Therefore, both TEM and MT soundings must be conducted at the same sounding site with a small distance between them and the TEM sounding used for static shift correction of the MT data.
- Though the static shift factor indicates the amount of difference between the TEM and MT curves, we can use it indirectly to determine near surface resistivity changes. Also those near surface resistivity changes can indicate near surface fluid circulation and alteration patterns.
- The TEM method is very reliable and less susceptible to close surface conductivities. Therefore, near surface resistivity distribution can be interpreted correctly (Figures 29, 31). The resistivity cross-section for profile for P1 (Figure 29) shows a low-resistivity cap (< 10 Ωm) underlain by a resistive body (high-resistivity core with a value of around 100 Ωm). Joint inversion of the data also expresses a low-resistivity layer cap at shallow depth. Another low-resistive body at depth, bounded within the high-resistive core, clearly domes up to two kilometres depth b.s.l. Roots of that intrusive body are displayed at 10 km depth b.s.l. (Figure 35). This low-resistivity body may indicate the heat source of the geothermal system.
- In the resistivity cross-section of profile P2, the heat source can be identified below 4 km b.s.l., but it is not as confined as in profile P1. Iso-resistivity maps address lateral resistivity changes. At 300 m a.s.l. and 0 m, maps indicate a clearly bounded low-resistive area. This also agrees with surface manifestation locations.
- Z-strike and T-strike (Tipper) maps show good correlation with the regional fracture pattern in 0.01-1.0 S. The data from this period represent up to 1-2 km depths. Below that (period 1-100 S), the tipper and Z-strike change direction. Due to these changes, we can conclude that the electrical strike direction changes suddenly and the resistivity structure marks a boundary.

- Comparison of the mineralogical sequence from a borehole with the resistivity cross-section P1 shows a fair match, even though the borehole is about 600 m away from the profile. The conductive zeolite and smectite zone appears within the low-resistivity cap and the more resistive chlorite/epidote appears within the high-resistivity core.
- Assuming all the above facts and evidence, it can be concluded that the resistivity and mineralogy evidence correlate fairly well with one another.

ACKNOWLEDGEMENTS

It is my pleasure to express my gratitude to the UNU-GTP for awarding this opportunity to participate in the six month UNU Geothermal Training Programme. The study and use of geothermal energy in Sri Lanka is very new. This programme not only provided my country with a knowledgeable professional, it also contributed a vast amount of knowledge to our research and exploration community.

My special thanks are offered to Dr. Ingvar Birgir Fridleifsson, the director, Mr. Lúdvík S. Georgsson, Ms. Thórhildur Ísberg, Mr. Ingimar G. Haraldsson and Mr. Markús A.G. Wilde, and all of UNU staff for their coordination of the training activities. Special thanks to my supervisors, Mr. Knútur Árnason, Mr. Gylfi Páll Hersir and Mr. Andemariam Teklesenbet Beyene for their superb guidance and assistance. I would like to thank all geophysical exploration fellows for sharing their knowledge and experience. Also I would like offer my special thanks to Eriya Kahwa for sharing his processed data for the final resistivity map preparations.

I am thankful to my employer, the Institute of Fundamental Studies, Sri Lanka and the Ministry of Technology and Research for granting me study leave for this six month training period. Many thanks go to my supervisor, senior research fellow Dr. N.D. Subasinghe for encouraging me to improve my proficiency in geothermal exploration and to my colleague, Mr. Thusitha Nimalsiri, for covering all my duties during my absence.

Finally, I would like to express my heartfelt thanks to my fiancée, Asiri Anushka, and my family, for giving me strength to keep up my studies while away from home.

REFERENCES

Árnason, K., 1989: *Central loop transient electromagnetic sounding over a horizontally layered earth.* Orkustofnun, Reykjavík, report OS-89032/JHD-06, 129 pp.

Árnason, K., 2006a: *TemX Short manual*. ÍSOR – Iceland GeoSurvey, Reykjavík, manual, 17 pp.

Árnason, K., 2006b: *TEMTD, a program for 1D inversion of central-loop TEM and MT data*. Short manual. ÍSOR – Iceland GeoSurvey, Reykjavík, manual, 17 pp.

Árnason, K., 2008: *The magnetotelluric static shift problem*. ISOR - Iceland GeoSurvey, Reykjavík, report ÍSOR-08088, 16 pp.

Cagniard, L., 1953: Basic theory of the magneto-telluric method of geophysical prospecting. *Geophysics, 18,* 605-635.

Christensen, A., Auken, E., and Sørensen, K., 2006: The transient electromagnetic method. *Groundwater Geophysics, 71*, 179-225.

Dakhnov, V.N., 1962: *Geophysical well logging*. Q. Colorado Sch. Mines, 57-2, 445 pp.

Deer, W.A., Howie, R.A., and Zussman, J., 1962: *Rock-forming minerals, vol. 3. Sheet silicates.* Longmans, Green and Co. Ltd., London, 270 pp.

DeGroot-Hedlin, G., 1991: Removal of static shift in two dimensions by regularized inversion. *Geophysics, 56,* 2102-2106.

Eysteinsson, H., 1998: *TEMRESD, TEMMAP and TEMCROSS plotting programs*. ÍSOR-Iceland GeoSurvey, unpublished programs and manuals.

Flóvenz, Ó.G., Hersir, G.P., Saemundsson, K., Ármannsson, H., and Fridriksson, T., 2012: Geothermal energy exploration techniques. In: Sayigh, A. (ed.), *Comprehensive renewable energy*, *Vol. 7*. Elsevier, Oxford, 51-95.

Franzson, H., 2008: Chemical transport in geothermal systems in Iceland: Evidence from hydrothermal alteration. *J. Volcanology & Geothermal Research, 173,*217-229.

Gíslason, G., Johnsen, G.V., Ármannsson, H., Torfason, H., and Árnason, K., 1984: Theistareykir. *Surface exploration of the high-temperature geothermal area.* Orkustofnun, Reykjavík, report OS84089/JHD16 (in Icelandic), 134 pp.

Hersir, G.P., and Björnsson, A., 1991: *Geophysical exploration for geothermal resources. Principles and applications*. UNU-GTP, Iceland, report 15, 94 pp.

Kahwa, E., 2012: Geophysical exploration of high-temperature geothermal areas using resistivity methods – case study: Theistareykir area, NE-Iceland. Report 14 in: *Geothermal training in Iceland 2012*. UNU-GTP, Iceland, 235-263.

Morgan, W.J., 1971: Convection plumes in the lower mantle. *Nature, 230*, 42-43.

Ogawa, Y., and Ushida, T., 1996: A two-dimensional magnetotelluric inversion assuming Gaussian static shift. *Geophys. J. Int., 126*, 69-76.

Quist, A.S., and Marshall, W.L., 1968: Electrical conductances of aqueous sodium chloride solutions from 0 to 800°C and at pressures to 4000 bars. *J. Phys. Chem., 72*, 684-703.

Pytte, A.M., and Reynolds, R.C., 1989: The thermal transformation of smectite to illite. In: Naeser, N.D., and McCulloh, T.H. (eds.), *Thermal history of sedimentary basins: Methods and case histories.* Springer-Verlag, NY, 133-140.

Saemundsson, K., 2007: *The geology of Theistareykir.* ÍSOR – Iceland GeoSurvey, Reykjavík, report ÍSOR-07270 (in Icelandic), 23 pp.

Schilling, J.-G., Meyer, P.S., and Kingsley R.H., 1982: Evolution of the Icelandic hotspot. *Nature, 296*, 313-320.

Simpson, F., and Bahr, K., 2005: *Practical magnetotellurics*. Cambridge University Press, Cambridge, UK, 254 pp.

Slater, L., McKenzie, D., Grönvold, K., and Shimizu, N., 2001: Melt and movement beneath Theistareykir, NE Iceland. *J. Petrology*, 42, 321-354.

Sternberg, B.K., Washburn, J.C., and Pellerin, L., 1988: Correction for the static shift in magnetotellurics using transient electromagnetic soundings. *Geophysics*, 53-11, 1459-1468.

Suriyaarachchi, N.B., 2012*: Appendices to the report "Joint 1D inversion of MT and TEM resistivity data from the Theistareykir high-temperature geothermal area, NE-Iceland and comparison with alteration and temperature logs from boreholes"*. UNU-GTP, Iceland, report 32 appendices, 27 pp.

Tikhonov, A.N., 1950: *Determination of the electrical characteristics of the deeper strata of the earth's crust*. Dokl. Akad. Nauk, USSR, 7-2.

Tucker, M.E., 1991: *Sedimentary petrology* (2nd ed.). Blackwell Scientific Publ., London, 260 pp.

Ward, S.H, and Wannamaker, P.E., 1983: *The MT/AMT electromagnetic method in geothermal exploration*. UNU-GTP, Iceland, report 5, 107 pp.